2012

Organic Radical Contrast Agents for Magnetic Resonance Imaging

Andrzej Rajca
University of Nebraska - Lincoln, arajca1@unl.edu

Ying Wang
University of Nebraska-Lincoln

Michael Boska
University of Nebraska Medical Center

Joseph T. Paletta
University of Nebraska-Lincoln

Arnon Olankitwanit
University of Nebraska - Lincoln

See next page for additional authors

Published in final edited form as:
J Am Chem Soc. 2012 September 26; 134(38): 15724–15727. doi:10.1021/ja3079829.

Organic Radical Contrast Agents for Magnetic Resonance Imaging

Andrzej Rajca[†,*], **Ying Wang**[†], **Michael Boska**[#], **Joseph T. Paletta**[†], **Arnon Olankitwanit**[†], **Michael A. Swanson**[‡], **Deborah G. Mitchell**[‡], **Sandra S. Eaton**[‡], **Gareth R. Eaton**[‡], and **Suchada Rajca**[†]

[†]Department of Chemistry, University of Nebraska, Lincoln, NE 68588-0304

[#]Department of Radiology, University of Nebraska Medical Center, Omaha, NE 68198

[‡]Department of Chemistry and Biochemistry, University of Denver, Denver, CO 80208-2436

Abstract

We report a molecular design that provides an intravenously injectable organic radical contrast agent (ORCA) that has molecular $r_1 \approx 5\ mM^{-1}s^{-1}$. The ORCA is based on spirocyclohexyl nitroxide radicals and polyethylene glycol chains conjugated to a generation 4 polypropylenimine dendrimers scaffold. The metal-free ORCA has a long shelf-life and provides selectively enhanced MRI in mice for over 1 h.

Paramagnetic organic radicals, such as stable nitroxides, have been investigated as magnetic resonance imaging (MRI) contrast agents.[1–6] Metal-free, organic radical contrast agent (ORCA) would provide an alternative to gadolinium-based contrast agents (GBCAs), which are the most widely used paramagnetic metal ion-based agents in the clinic. Although GBCAs are well tolerated by the majority of patients, patients with impaired kidney function are reported to be at increased risk of developing a serious adverse reaction named nephrogenic systemic fibrosis (NSF).[7] Since the first report on this adverse effect in renal-dialysis patients and its association with gadolinium,[8,9] guidelines on the administration of GBCAs have been issued and implemented worldwide to minimize the risk for NSF.

To date, the critical obstacle in the development of a practical ORCA for MRI is the design and synthesis of paramagnetic compounds of moderate molecular size that possess long *in vivo* lifetime, high ^1H water relaxivity (r_1), and high water solubility.[1–6]

Commonly used, paramagnetic nitroxides undergo fast reduction *in vivo*, especially in the bloodstream and tissues, to diamagnetic hydroxylamines.[2,3] For example, 3-carboxy-2,2,5,5-tetramethyl-l-pyrrolidinyloxy (3-CP) (Scheme 1) and its derivatives, which are among the most widely used and most resistant to reduction nitroxide radicals, have a short half-life (ca. 2 min) in the bloodstream and kidneys, as determined by MRI mouse studies.[2,3] Although nitroxides with one unpaired electron, total spin quantum number, $S = ½$, possess low ^1H water relaxivity,[10] e.g. $r_1 \approx 0.15\ mM^{-1}s^{-1}$ at 7 T for 3-CP, they have been utilized as functional redox-sensitive agents in MRI studies, and as *in vivo* radioprotectors. [2,3,11] In

Corresponding Author: arajca1@unl.edu.

Notes

The authors declare no competing financial interests.

Supporting Information

Materials, general methods, instrumentation, synthetic protocols, *in vitro* and *in vivo* characterizations. This material is available free of charge via the Internet at http://pubs.acs.org.

principle, r_1 could be increased by conjugation of paramagnetic metal chelates or radicals to rigid scaffolds.[12–14] However, previous examples of conjugation of nitroxides to dendrimers did not provide increased r_1,[15,16] as shown in the case of the generation 3 (G3) polypropylenimine (PPI) dendrimers conjugated with nitroxides 3-CP which has $r_1 \approx 0.16$ $mM^{-1}s^{-1}$ at 1.5 T, similar to that for common nitroxides. Despite low r_1 and low solubility in water,[15] *in vivo* MR images of the rabbit stifle joints, obtained by intraarticular administration of these agents, showed significant enhancement of articular cartilage in T_1-weighted images.[1] Fast reduction and low r_1 of nitroxides pose serious obstacles because they severely limit available MR imaging time and contrast, while increasing dose of the agent to compensate for reduction and low r_1 could lead to oxidative stress.[17] A practical ORCA, especially suitable for intravenous injection, remains elusive.

We report a water-soluble ORCA with long *in vivo* lifetime and high r_1 that provide selectively enhanced MRI in mice for over 1 h.

Our approach to the design of ORCA relies on spirocyclohexyl nitroxide radical **1**-OH (Figure. 1). The 5-membered ring (pyrrolidinyl) nitroxide radical[18,19] that is sterically shielded[20] by the spirocyclohexyl groups[21] is expected to be reduced at a slower rate *in vivo*, particularly by antioxidants such as ascorbate (vitamin C). Through judicious molecular design, conjugation of nitroxide radicals to a rigid scaffold should provide an agent with not only increased resistance to reduction but also with increased relaxivity. We consider dendrimers (branched structures), which have been demonstrated to be more effective as scaffold for linking Gd-chelates than linear structures in the approaches to increased relaxivity of GBCAs.[13,14,22] Because hydrophobicity of nitroxide- covered dendrimer surface may contribute to limited applications of the agents in MRI, our approach is aimed at alleviating that effect by including water solubilizing groups such as polyethylene glycol (PEG) chains on the surface of the dendrimer. The non-immunogenic and polar PEG chains may provide additional advantages,[23] that is, the PEG chains may help to immobilize nitroxides as well as increase water access to the paramagnetic nitroxides that could help to increase r_1. Our design strategy is to optimize the ratio of nitroxide and PEG chains on the dendrimer surface to obtain ORCA with high r_1 and good water solubility. This concept is tested using PPI dendrimer conjugated with spirocyclohexyl nitroxide **1** and hydrophilic, monodisperse methoxypolyethylene glycol (mPEG-12) chains to obtain water soluble ORCA.

The spirocyclohexyl nitroxide **1**-OH is synthesized by modification of methods for 3-CP,[24] and then the carboxylic acid is converted to *N*-hydroxysuccinimidyl (NHS) ester, **1**-NHS, using standard methods. Sequential conjugation of **1**-NHS, and mPEG-12-NHS to PPI dendrimer generation-4 (PPI-G4) with 64 terminal amine groups ($(NH_2)_i$, $i = 64$) provides ORCA **1**-mPEG-G4. Through tests of various reaction conditions, it was determined that using about 1/3 stoichiometric amount (1/3 equiv) of **1**-NHS and an excess of 2/3 equiv of mPEG-12-NHS is optimum. The resultant **1**-mPEG-G4 has water solubility ≥0.5 g/mL and radical concentration ≥0.4 mmol/g. ORCAs **1**-mPEG-G3, **1**-mPEG-G2, and **1**-mPEG-G0, as well as 3-CP-mPEG-G4 are prepared by analogous procedure (Table 1).

The number of conjugated spirocyclohexyl nitroxide **1** and mPEG-12 moieties per PPI dendrimer core is determined using end group analysis based upon ^{1}H NMR spectroscopy and spin counting by EPR spectroscopy. Because ^{1}H NMR spectra of paramagnetic ORCAs are broad, and not useful for characterization, we convert the nitroxides to diamagnetic hydroxylamines by treating the ORCAs with excess of ascorbate. The partially reduced ORCAs provide sufficiently well resolved ^{1}H NMR spectra for determination of the number of conjugated mPEG-12 (m), by the relative integrals of ^{1}H resonances for the terminal methyl groups of mPEG-12 and the ^{1}H resonances of the dendrimer scaffold. Spin counting

provides the spin concentration of the ORCA sample (prior to treatment with ascorbate), which can be used to determine the number of conjugated nitroxide radicals (*j*). The PPI dendrimer surface coverage determined from the values of *m* and *j* is shown in Table 1. For **1**-mPEG-G4, about 80% of the dendrimer surface is covered with nitroxides **1** and mPEG-12 and this surface coverage increases to about 90% for lower generations of ORCA. This incomplete surface coverage may be associated with well-known overcrowding on the surfaces of the higher generation dendrimers[25] that is further amplified by larger space requirements of spirocyclic nitroxide vs. mPEG-12, as illustrated by the surface coverage of 64% and 92% for model compounds **1**-G4 and mPEG-G4. Covalent attachment of both mPEG-12 and the reduced nitroxides (hydroxylamines) to the scaffold is evidenced by two broad ^{1}H NMR peaks at δ 7.9 and δ 10.4 ppm (dimethylsulfoxide-d^6), assigned to two distinct NH amide groups. mPEG-G4 has only one type of NH amide group (singlet at δ 7.9 ppm), which shows a ^{1}H-^{1}H COSY cross-peak to the dendrimer backbone (Figures S10–S18).

We investigate the rate of reduction of nitroxides **1**-OH and ORCA **1**-mPEG-G4 under pseudo-first order conditions using 20-fold excess ascorbate in pH 7.4 PBS buffer. As reference, the rate of reduction of 3-CP is determined under identical conditions. Second order rate constants, *k*, are obtained by following the decay of the nitroxide EPR peak height at 295 K (Figure 2A).

The spirocyclohexyl nitroxide, **1**-OH ($k = 0.031 \pm 0.003$ $M^{-1}s^{-1}$) is reduced at a significantly slower rate than 3-CP ($k = 0.063 \pm 0.002$ $M^{-1}s^{-1}$).[19] Under similar conditions, initial reduction of **1**-mPEG-G4 occurs with the rate constant, $k = 0.058 \pm 0.004$ $M^{-1}s^{-1}$, which is comparable to that of 3-CP. However, after a fraction of nitroxides is reduced during the initial 1-h period, the remaining nitroxides **1** on the crowded dendrimer surface are reduced at about 20-fold slower rate (Table S2).

^{1}H water relaxivity r_1 of ORCAs and 3-CP in PBS buffer are measured using a 7-T MRI scanner. The plots of $1/T_1$ (^{1}H relaxation rate of water) vs. nitroxide concentration are linear for all agents, indicating the absence of aggregation in the concentration range studied, 0–16 mM (per-nitroxide) (Fig. 2B). The slopes of the plots indicate that, under physiological conditions (PBS, pH 7.2), ^{1}H water relaxivity of PEGylated ORCAs is significantly higher than for 3-CP. For example, $r_1 = 0.42 \pm 0.03$ $mM^{-1}s^{-1}$ per $S = ½$ nitroxide radical in **1**-mPEGG4, corresponding to molecular $r_1 \approx 5$ $mM^{-1}s^{-1}$, may be compared to 3-CP with $r_1 \approx 0.14$ $mM^{-1}s^{-1}$ (Table 1). Solutions of **1**- mPEG-G4 in PBS buffer are stable at room temperature, with r_1 showing negligible change over 24 h; similarly, no change is detected in spin concentration by EPR spectroscopy for **1**- mPEG-G4 in PBS buffer stored at −20 °C for 5 months.

We examine rotational dynamics of the ORCA by EPR line-shape analysis. Because high spin concentration leads to exchange broadening of EPR spectra, we decrease spin concentration of ORCA, by treatment with ascorbate in PBS buffer, to obtain adequately resolved EPR spectra for the analysis. Simulations of the EPR spectra of the partially reduced ORCAs provide rotational correlation time (τ_{rot}) in the ns-range (Table 1), compared to $\tau_{rot} = 0.045$ ns for 3-CP under identical conditions. The value of τ_{rot} for **1**-mPEG-G4 is about 50% longer than that for 3-CP-mPEG-G4, emphasizing the effectiveness of the spirocyclohexyl, and thus more rigid, structure of nitroxide **1** in restricting the motion of the radical. Although the ORCA with the longest $\tau_{rot} = 1.5 \pm 0.1$ ns possesses the highest r_1, the relaxivity is only weakly dependent on τ_{rot}. This suggests the possibility of different factors limiting r_1 for the ORCAs, such as short electron spin relaxation time T_{1e} and long residence/exchange time (τ_{exch}) of water molecule hydrogen-bonded to the nitroxide radical.

EPR line-shape analyses for **1**-mPEG-G4, -G3, and -G2 suggest that T_{1e} is longer than about 20 ns, based upon the assumption $T_{1e} > T_{2e}$ estimated from linewidths. Because the dominant mechanism for shortening of T_{1e} is by the modulation of electron-electron spin-spin interaction by motion,[26] the highly restricted motion of the radicals in the ORCAs ($\tau_{rot} \approx 1$ ns) is likely to prevent T_{1e} from becoming sufficiently short, to affect water r_1 significantly (Figure S22). This leaves long τ_{exch} as the most probable factor limiting water r_1, similar to the behavior observed in conjugates of Gd-chelates with dendrimers.[27] The dipolar inner sphere model,[28] which is the standard in the analysis of Gd-chelates,[13,22] predicts that shortened $\tau_{exch} \leq 1$ μs, i.e., improved access of water to radicals, should facilitate increased water r_1. For example, $r_1 \approx 5$ $mM^{-1}s^{-1}$ per $S = ½$ nitroxide radical is computed for $\tau_{exch} \approx 1$ μs, $\tau_{rot} \approx 1.5$ ns, and $T_{1e} \geq 20$ ns (Figure S22).

To explore the potential of ORCAs as practical MRI contrast agents, we investigate **1**-mPEG-G4 *in vivo*. Since the r_1 per $S = ½$ nitroxide radical for **1**-mPEG-G4 is about 3 times higher than for a typical nitroxide, we used a relatively small dose of radical, 0.5 mmol/kg, which is 3 times less than the typical dose for common nitroxides in *in vivo* MRI studies.[2,3] The T_1 weighted high resolution 3D images of the mouse torso show that the **1**-mPEG-G4 is a long lasting blood pool contrast agent, which is slowly excreted through the kidneys (Figures 3, 4, and Fig. S25). This can be appreciated in the subtraction images shown in Figure 3B–D, F–H. It is clear that the liver and spleen show no appreciable uptake, only residual signal as a result of the vasculature, while the lung, normally a low intensity organ in MRI, lights up due to the enhancement of the vasculature.

The MRI signal in blood and kidneys decays gradually allowing for a long imaging time. For example, the image enhancement (mean ± standard deviations, n = 3) in kidneys medulla and blood vessels is 114 ± 14% and 81 ± 27% after 30 min following administration of the agent and slowly decreases to 104 ± 11% and 60 ± 26% after 90 min of scanning, respectively (Figure 4).

Although the present data do not allow for quantitation of the excretion of the agent, selective uptake by the kidneys medulla and cortex, and the enhanced image of the bladder (Figure 3), suggest excretion of ORCA through the kidneys. ORCA **1**-mPEG-G4, with average $M_n \approx 32$ kDa (Table 1), is estimated to have a Stokes-Einstein radius (r_{SE}) of about 2.4 nm, which is near the upper limit, $r_{SE} \approx 2.5$ nm, for glomerular filtration of positively charged spherical solutes,[29] and could thus account for strongly enhanced MR image of kidneys, especially medulla, over a period exceeding 1 h (Table 1).

Supplementary Material

Refer to Web version on PubMed Central for supplementary material.

Acknowledgments

We thank Drs. Przemysław J. Boratyński and Krzysztof Waskiewicz for preliminary synthesis of **1**-mPEG-G4. This research was supported by NSF CHE-1012578 (UNL), NIH NIBIB EB008484 (UNL), Nebraska Research Initiative (UNL and UNMC), and NIH NIBIB EB002807 (Denver).

References

1. Winalski CS, Shortkroff S, Schneider E, Yoshioka H, Mulkern RV, Rosen GM. Osteoarthritis and Cartilage. 2008; 16:815–822. [PubMed: 18226558]
2. Hyodo F, Matsumoto K, Matsumoto A, Mitchell JB, Krishna MC. Cancer Res. 2006; 66:9921–9928. [PubMed: 17047054]

3. Davis RM, Matsumoto S, Bernardo M, Sowers A, Matsumoto K, Krishna MC, Mitchell JB. Free Rad Biol Med. 2011; 50:459–468. [PubMed: 21130158]
4. Utsumi H, Yamada K, Ichikawa K, Sakai K, Kinoshita Y, Matsumoto S, Nagai M. Proc Natl Acad Sci U S A. 2006; 103:1463–1468. [PubMed: 16432234]
5. Gallez B, Lacour V, Demeure R, Debuyst R, Dejehet F, De Keyser JL, Dumont P. Magn Reson Imag. 1994; 12:61–69.
6. Brasch RC, London DA, Wesbey GE, Tozer TN, Nitecki DE, Williams RD, Doemeny J, Tuck LD, Lallemand DP. Radiology. 1983; 147:773–779. [PubMed: 6844613]
7. Braverman IM, Cowper S. F1000 Med Reports. 2010; 2:84. http://f1000.com/reports/m/2/84. 10.3410/M2-84
8. Grobner T. Nephrol Dial Transplant. 2006; 21:1104–1108. [PubMed: 16431890]
9. Marckmann P, Skov L, Rossen DA, Damholt MB, Heaf JG, Thomsen HS. J Am Soc Nephrol. 2006; 17:2359–2362. [PubMed: 16885403]
10. Vallet P, Van Haverbeke Y, Bonnet PA, Subra G, Chapat JP, Muller RN. Magn Reson Med. 1994; 32:11–15. [PubMed: 8084224] S = 1 nitroxide diradicals have similarly low r_1 (per nitroxide moiety): Spagnol G, Shiraishi K, Rajca S, Rajca A. Chem Commun. 2005:5047–5049.
11. Davis RM, Sowers AL, DeGraff W, Bernardo M, Thetford A, Krishna MC, Mitchell JB. Free Radical Biol Med. 2011; 51:780–790. [PubMed: 21664459]
12. Chan HC, Sun K, Magin RL, Swartz HM. Bioconjugate Chem. 1990; 1:32–36.
13. Villaraza AJL, Bumb A, Brechbiel MW. Chem Rev. 2010; 110:2921–2959. [PubMed: 20067234]
14. Floyd WC III, Klemm PJ, Smiles DE, Kohlgruber AC, Pierre VC, Mynar JL, Fréchet JMJ, Raymond KN. J Am Chem Soc. 2011; 133:2390–2393. [PubMed: 21294571]
15. Winalski CS, Shortkroff S, Mulkern RV, Schneider E, Rosen GM. Magn Res Med. 2002; 48:965–972.
16. Francese G, Dunand FA, Loosli C, Merbach AE, Decurtins S. Magn Reson Chem. 2003; 41:81–83.
17. Silberstein T, Mankuta D, Shames AI, Likhtenshtein GI, Meyerstein D, Meyerstein N, Saphier O. Archives of Gynecology and Obstetrics. 2008; 277:233–237. [PubMed: 17713779]
18. Keana JF, Pou S, Rosen GM. Magn Reson Med. 1987; 5:525–536. [PubMed: 3437813]
19. Vianello F, Momo F, Scarpa M, Rigo A. Magn Reson Imaging. 1995; 13:219–226. [PubMed: 7739363]
20. Bobko AA, Kirilyuk IA, Grigor'ev IA, Zweier JL, Khramtsov VV. Free Radical Biol Med. 2007; 42:404–412. [PubMed: 17210453]
21. Kirilyuk IA, Polienko YF, Krumkacheva OA, Strizhakov RK, Gatilov YV, Grigor'ev IA, Bagryanskaya EG. J Org Chem. 2012; 77 ASAP: 08/23/2012. 10.1021/jo301235j
22. Caravan P. Chem Soc Rev. 2006; 35:512–523. [PubMed: 16729145]
23. Joralemon MJ, McRae S, Emrick T. Chem Commun. 2010; 46:1377–1393.
24. Sosnovsky G, Cai Z. J Org Chem. 1995; 60:3414–3418.
25. Newkome, GR.; Moorefield, CN.; Vögtle, F. Dendrimers and Dendrons. Wiley-VCH; Weinheim: 2001. p. 1-623.
26. Sato H, Kathirvelu V, Spagnol G, Rajca S, Rajca A, Eaton SS, Eaton GR. J Phys Chem B. 2008; 112:2818–2828. [PubMed: 18284225]
27. Nicolle GM, Toth E, Schmitt-Willich H, Raduchel B, Merbach AE. Chem Eur J. 2002; 8:1040–1048. [PubMed: 11891890]
28. Maliakal AJ, Turro NJ, Bosman AW, Cornel J, Meijer EW. J Phys Chem A. 2003; 107:8467–8475.
29. Haraldsson B, Sörensson J. Physiology. 2004; 9:7–10.

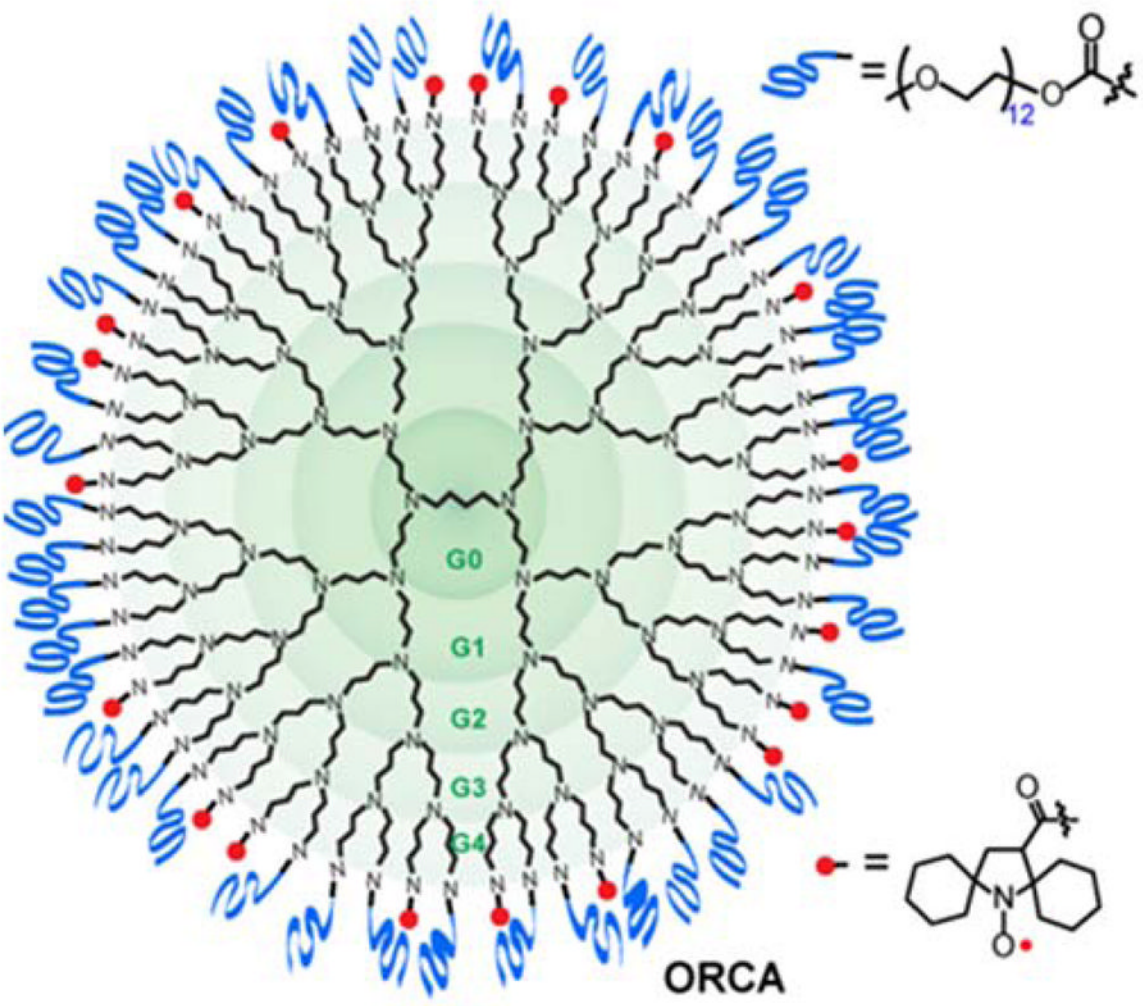

Figure 1.
Organic radical contrast agent (ORCA).

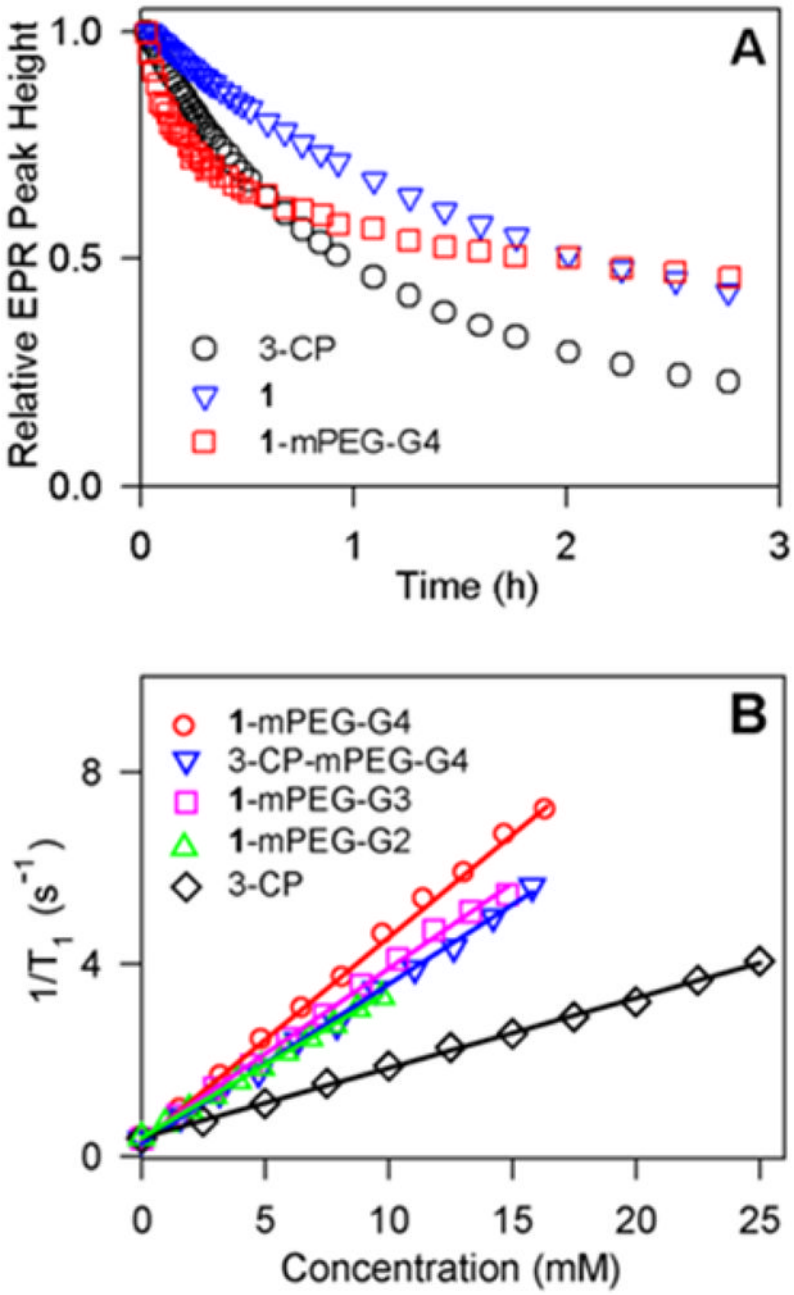

Figure 2.

(**A**) Reduction of 0.2 mM nitroxide radicals with 4 mM ascorbate in 125 mM PBS pH 7.4 at 295 K. (**B**) Plots of water ^{1}H relaxation rates, $1/T_1$, vs. concentration of nitroxide radicals in PBS pH 7.2; water relaxivities r_1 determined from slopes of the linear fits (R^2 = 0.998–0.999).

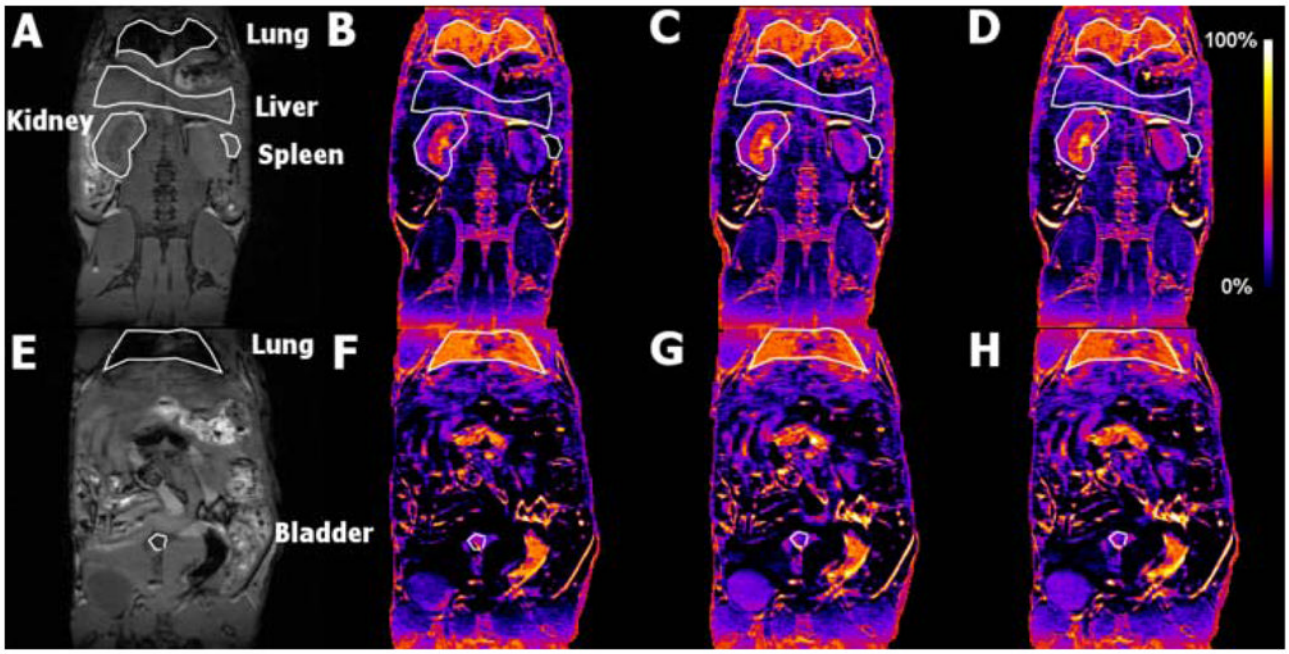

Figure 3.
3D T1 weighted spoiled gradient recalled echo MRI of mouse before and after injection of **1**-mPEG-G4. (A,E) MRI before injection and (B–D,F–H): subtraction of preinjection images from images obtained (B,D) 0–30 min, (C,E) 30–60 min, and (D,H) 60–90 min after injection.

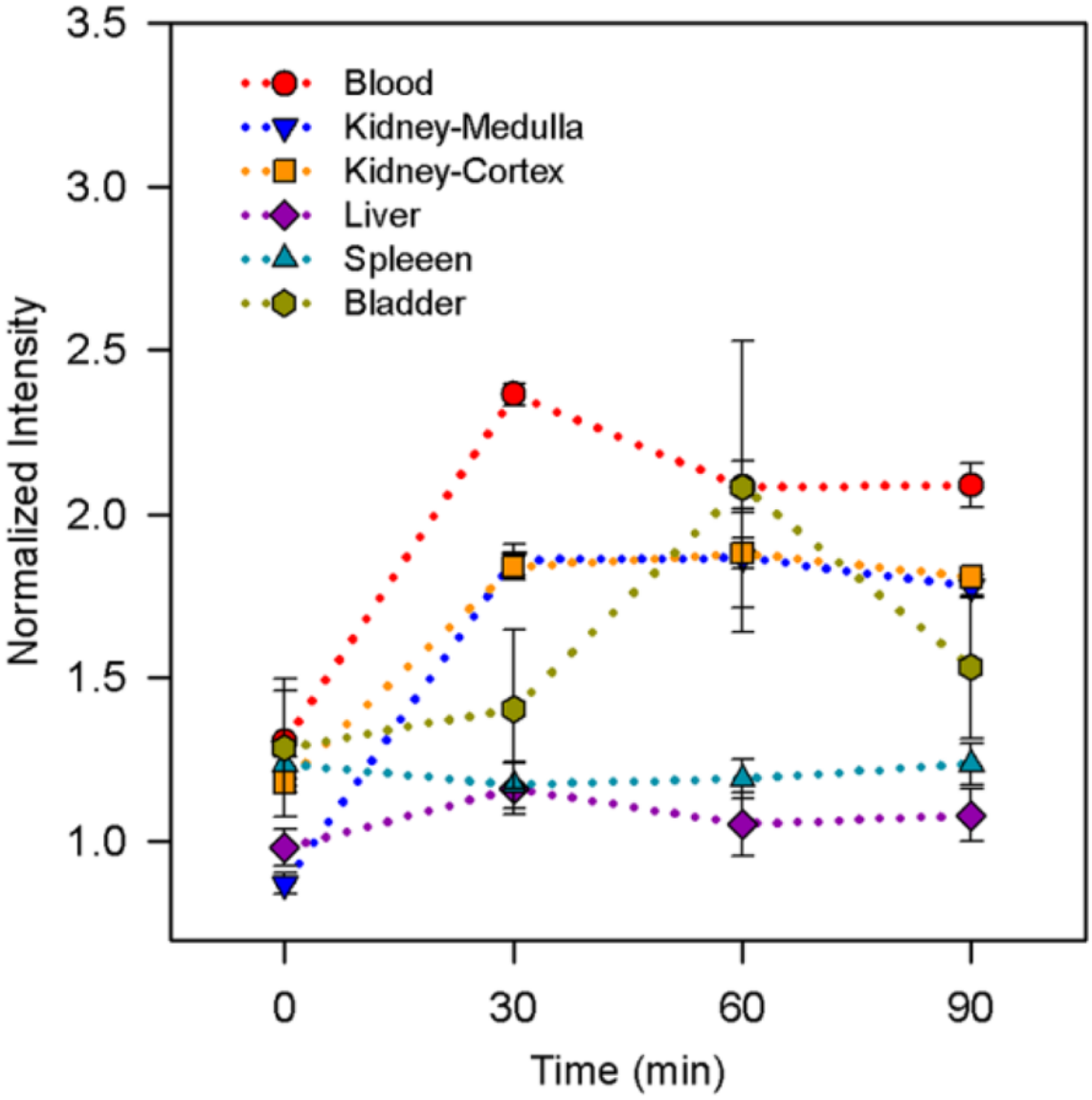

Figure 4.
Plots of normalized intensities (mean ± standard errors, n = 3) before and after injection of **1**-mPEG-G4.

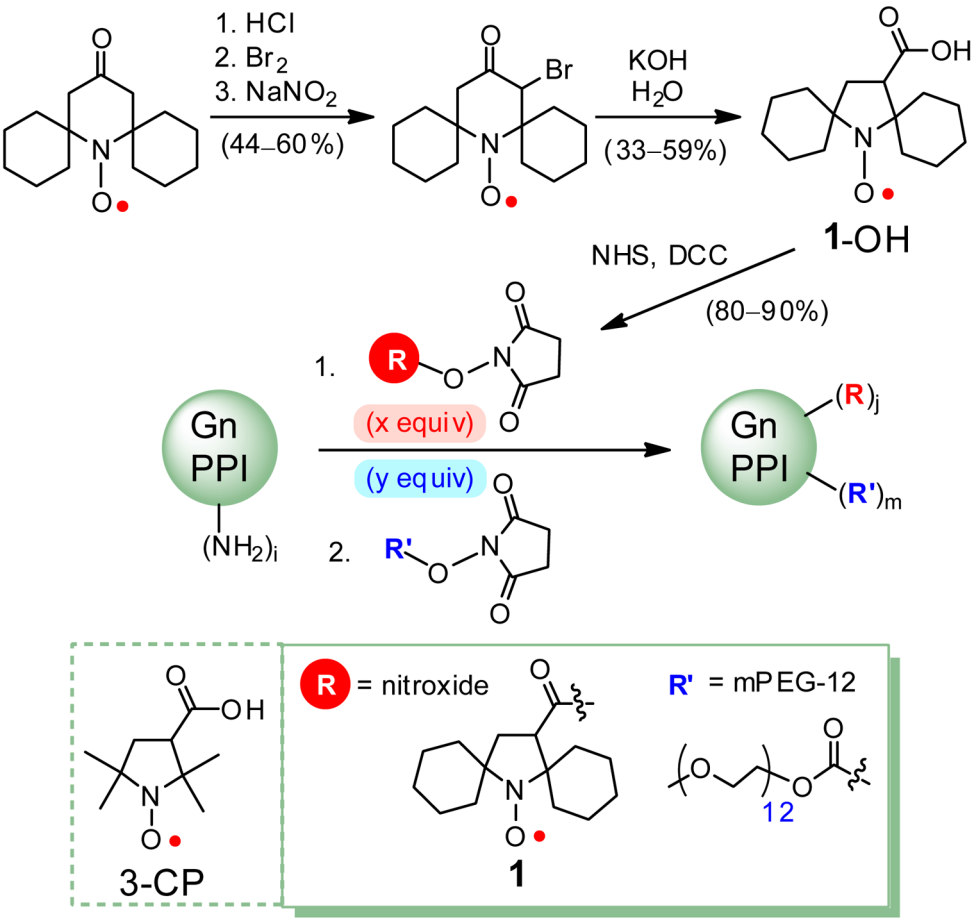

Scheme 1.

Table 1

Summary of ORCAs.

PPI	*i*	ORCA	x (equiv)	y (equiv)	Spin Conc. (mmol g^{-1})	r_1 ($mM^{-1}s^{-1}$)[a]	τ_{rot} (ns)	*j*	*m*	$(R')_m/(R)_j$	Surface Coverage (%)	M_n (kDa)
G4	64	**1**-mPEG-G4	21–22	54–65	0.41 ± 0.01	0.42 ± 0.03	1.5 ± 0.1	13.1 ± 0.5	37.9 ± 2.0	2.90 ± 0.04	79.6 ± 4.0	32
G3	32	**1**-mPEG-G3	11	25	0.46 ± 0.01	0.37 ± 0.02	0.84 ± 0.06	8	20	2.5	86	17
G2	16	**1**-mPEG-G2	6	15	0.46 ± 0.04	0.29 ± 0.02	0.49 ± 0.02	4	10	2.5	90	8.4
		1-G4	70–80	0	2.36 ± 0.03	-	-	41 ± 1	0	0	64 ± 2	17
G4	64	mPEG-G4	0	70	0	-	-	0	59	-	92	41
		3-CP-mPEG-G4	21	52	0.50 ± 0.05	0.33	0.85 ± 0.07	-	-	-	-	-
		3-CP	-	-	-	0.14	0.045	-	-	-	-	-

[a] r_1 ($mM^{-1}s^{-1}$): mM^{-1} of $S = ½$ nitroxide radical (per $S = ½$ nitroxide radical); *i* is number of NH_2 groups; x and y are molar equivalents of nitroxide- NHS and mPEG-12-NHS; *j* and *m* are number of conjugated nitroxide radicals (R) and mPEG-12 (R′) - see Scheme 1.

Supporting Information

Organic Radical Contrast Agents for Magnetic Resonance Imaging

Andrzej Rajca[1], Ying Wang[1], Michael Boska[2], Joseph T. Paletta[1], Arnon Olankitwanit[1], Michael A. Swanson,[3] Deborah G. Mitchell,[3] Sandra S. Eaton[3], Gareth R. Eaton[3], Suchada Rajca[1]

[1]Department of Chemistry, University of Nebraska, Lincoln, NE 68588-0304.

[2]Department of Radiology, University of Nebraska Medical Center, Omaha, NE 68198.

[3]Department of Chemistry and Biochemistry, University of Denver, Denver, CO 80208-2436

Table of Contents

Section 1. Materials, General Methods, and Instrumentation

Note: Throughout the Supplementary Information, labels "yw0380B3" and alike correspond to sample or experiment codes directly traceable to the laboratory notebooks or raw data.

All solvents were distilled, e.g., dimethylformamide (distilled under vacuum from calcium hydride), toluene (freshly distilled from sodium), and THF (freshly distilled from sodium benzophenone), or alternatively, obtained from solvent purification system (LC Technology Solutions). *N*,*N*-Diisopropylethylamine (Hünig's base) was dried over calcium hydride, and then distilled. Per-deuterated solvents for NMR spectroscopy were obtained from Cambridge Isotope Laboratories or Aldrich and used as received. Monodisperse mPEG-12-NHS was obtained from Quanta BioDesign. All other commercially available chemicals were obtained from either Aldrich or Fisher, unless indicated otherwise. Column chromatography (0–20 psig pressure) was carried out on flash silica gel (Sorbent Technologies). Analytical and preparative glass plates (tapered with a preadsorbent zone) for thin layer chromatography (TLC) were obtained from Analtech. Standard techniques for synthesis under inert atmosphere, using Schlenk glassware and gloveboxes (Vacuum Atmospheres), were employed for synthesis of ORCA.

CW X-band EPR spectra for spin quantitation of nitroxide radicals and kinetics of reduction were acquired on a Bruker EMX instrument at Nebraska, equipped with a frequency counter and nitrogen flow temperature control (120–300 K). The spectra were obtained using a Bruker TE_{102} cavity. DPPH powder (g = 2.0037) was used as a g-value reference. The spin concentration of low molecular weight nitroxide radicals and of nitroxide radicals in ORCA were measured in dichloromethane and PBS buffer at room temperature (295 K), respectively; 4-oxo-TEMPO and/or 3-carboxy-PROXYL in respective solvents were used as intensity references. For low molecular weight nitroxide radicals, typical parameters were: modulation amplitude, 0.2 G; sweep width, 100 G.

^{1}H NMR spectra were obtained with Bruker spectrometers (^{1}H, 600, 500, and 400 MHz) using chloroform-*d* ($CDCl_3$), water-d_2 (D_2O), dimethylsulfoxide-d_6 (DMSO-d_6), and acetone-d_6 as solvents. (Spectra obtained in per-deuterated PBS buffer are labeled as obtained in D_2O.) The chemical shifts were measured with respect to residual solvent peak of chloroform-*d* (δ 7.26 ppm), dimethylsulfoxide-d_6 (δ 2.50 ppm) and acetone-d_6 (δ 2.05 ppm); for spectra in D_2O or deuterated PBS buffer, the chemical shifts were referenced with respect to 0.05 wt% of 3-(trimethylsilyl) propionic-2,2,3,3-d_4 acid, sodium salt as the internal chemical shift standard (δ 0.00 ppm). IR spectra were obtained using a Nicolet Avatar 360 FT-IR instrument, equipped with an ATR sampling accessory (Spectra Tech, Inc.). A few drops of the solution were applied to the surface of a ZnSe ATR plate horizontal parallelogram (45°, Wilmad). After the solvent evaporated, the spectrum was acquired (typically at 2-cm^{-1} resolution). Mass spectra (MS) were obtained at the Nebraska Center for Mass Spectrometry. Low molecular weight nitroxides were analyzed by fast atom bombardment (FAB) MS, using 3-nitrobenzyl alcohol (3-NBA) or 1-(2-Nitrophenoxy)octane (Ortho-NitroPhenylOctylEther = ONPOE) as matrices, and electrospray ionization (ESI) MS, using sodium acetate in methanol/water.

Water was purified using a Nanopure Water System (Barnstead). Values of pH were measured using Corning pH/Ion Analyzer 350. Dialyses of ORCA were carried out using GeBAFlex tubes with a cut-off molecular weight of 3500 Daltons.

Section 2. Synthetic Protocols

2.a Synthesis of nitroxide radicals 1-OH and 1-NHS. Syntheses of **1** and **1**-NHS are summarized by the equations below, and described in detail in the remainder of this subsection. The starting nitroxide radical **2** was prepared according to the literature procedure[1,2]. Purity for all synthesized nitroxide radicals **2**-Br, **1**-OH, and **1**-NHS is confirmed by EPR spectroscopic spin concentrations (90–100%) and paramagnetic ^{1}H NMR spectra (Figs. S4, S7, and S8).

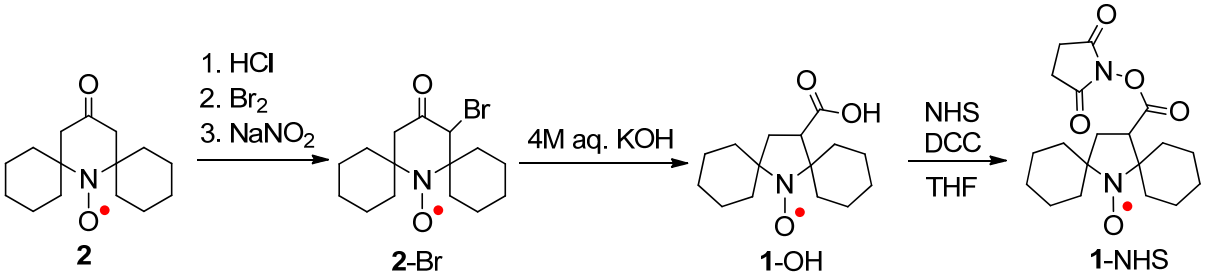

Protocol for nitroxide **2**-Br and its reduction to the corresponding hydroxylamine.

Run No.	SM (g/mmol) [mL of EtOH]	HCl (mL/mmol) [mL of conc. HCl diluted to 10 mL with EtOH]	Br_2 (mL/mmol)[a]	Bromination	1 M $NaNO_2$ in H_2O (mL/mmol)	Yield (g/%)	Spin Conc. (%)
1	1.000/4.00 [5.0]	2.4/5.2 [1.82]	3.65/4.0	3 min at -100 °C 25 min at r.t.	3.5/3.5	0.687/52	
2	0.917/3.67 [4.5]	2.3/4.8 [1.75]	2.01/3.7	3 min at -100 °C 25 min at r.t.	3.2/3.2	0.717/59	
3	2.933/11.7 [14]	7.4/15.5 [1.75]	5.5/11.9	3 min at -100 °C 30 min at r.t.	10.2/10.2	1.865/48	
4	1.618/6.46 [6.5]	4.0/8.4 [1.74]	4.0/6.5	3 min at -10 °C 30 min at r.t.	9/9	1.193/56	
5	1.395/5.57 [6.0]	3.7/7.7 [1.74]	3.7/6.0	3 min at -10 °C 30 min at r.t.	12/12	1.109/60	94
6	1.125/4.49 [4.6]	2.8/5.8 [1.74]	2.2/3.6	3 min at -10 °C 32 min at r.t.	10/10	0.652/44	

[a] 1 – 2 M solutions of Br_2 in $CHCl_3$

Procedure based on run no. 5. Our procedure is based upon previous report for bromination of 4-oxo-TEMPO to the corresponding bromo-nitroxide[3]. In a 25 mL conical flask, nitroxide radical **2** (1.395 g, 5.57 mmol) was suspended in ethanol (6.0 mL) and cooled in an ice water bath. A solution of HCl (3.7 mL, 7.73 mmol, 1.3 equiv, made by diluting 1.74 mL of concentrated HCl to 10 mL with ethanol) was added and briefly stirred, forming a yellow colloid. The reaction mixture was then stirred at room temperature for 90 min during which time the yellow colloid became white. The reaction mixture was then concentrated under a stream of nitrogen, evacuated, and charged with nitrogen. The resultant white solid was suspended in chloroform (4.2 mL), and cooled to –10 °C in an acetone/water ice bath, a solution of bromine in chloroform (3.7 mL, 6.0 mmol, 1.0 equiv, prepared by adding 5.0 mL of chloroform to 0.40 mL

of bromine) was added dropwise, forming a dark red solution. The reaction mixture stirred at –10 °C for 3 min, and then at room temperature for 30 min, over which time the solution became light brown. Then, an aqueous solution of $NaNO_2$ (1 M, 12 mL, 12 mmol, 2.0 equiv) was added and the reaction mixture immediately became dark brown and a brown gas was evolved. The reaction mixture was stirred at room temperature for 1 h, during which time the color became light orange. The reaction mixture was transferred to a separatory funnel with chloroform (100 mL) and washed with water (75 mL). The organic layer was dried over anhydrous $MgSO_4$ and concentrated with a rotatory evaporator. The crude (2.096 g) was dissolved in chloroform/hexanes (1:1), and then purified by column chromatography (silica gel, hexanes/ethyl ether, 6:1) Initially, a light yellow band, corresponding to an unknown by-product, is eluted, followed by the deep orange band of the product, which after evaporation of solvents, yields bromo-nitroxide **2**-Br as a crystalline orange solid (1.109 g, 60%). m.p. 83–86 °C. IR (ZnSe, cm^{-1}): 2927, 2858, 1717 (C=O), 1526, 1456, 1446, 1396, 1340, 1314, 1260, 1228, 1203, 1174, 1063, 925, 856, 736, 705. EPR (X-band): $g = 2.0067$, $a_N = 15.2$ G, spin concentration = 94% (1.0 mM in $CHCl_3$). LR FAB-MS (ONPOE, negative ions): *m*/*z* ion type (%RA = percent relative amplitude for *m/z* 240–750) 330.0 $[M+2H]^-$ (100%), 331.9 $[M+2+2H]^-$ (100%).

Reduction of bromo-nitroxide 2-Br to the corresponding hydroxylamine using phenylhydrazine. Bromo-nitroxide **2**-Br (2 mg) was dissolved in $CDCl_3$ and the ^1H NMR (400 MHz) spectrum was obtained (label: JTP-3-100f1_before). Then 6 drops of a solution of phenylhydrazine in $CDCl_3$ (3 drops of phenylhydrazine in 1 mL $CDCl_3$) was added and shaken for 10 minutes. The solution lost its orange color and nitrogen was evolved. ^1H NMR (400 MHz) was obtained (label: JTP-3-100f1_after) showing formation of the corresponding diamagnetic hydroxylamine (Fig. S6).

Protocol for nitroxide **1**-OH.

Run No.	SM (g/mmol)	KOH (mL/mmol)[a]	Reaction Time (h)	Yield (mg/%)
1	0.287/0.872	12/43.6	37	78/34
2	0.552/1.68	20/88.9	71	149/33
3	0.521/1.58	20/87.0	30	169/40
4	1.193/3.62	46/184	66	411/43
5	0.308/0.935	11.7/45.6	112	147/59

[a] 3.5 – 4.5 M solutions of KOH in water

Procedure based on run no. 5. Bromo–nitroxide **2**-Br (308 mg, 0.935 mmol) was suspended in aq. KOH (4 M, 11.7 mL, 46.8 mmol) and stirred for five days in darkness. After two days all starting material had dissolved giving a cloudy mixture with sticky red pieces of an unknown by product. After three days, the solution was clear but the sticky pieces were still present. After five days the reaction mixture was transferred to a separatory funnel and washed with chloroform (2 × 50 mL) removing a pink color. The separatory funnel and chloroform solution were cooled in water ice, then an aqueous solution of $NaHSO_4$ (1.5 M, 38 mL, 57 mmol) was added and immediately extracted with chloroform (6 × 100 mL). The chloroform extracts

were combined, washed with water (250 mL) and dried over anhydrous $MgSO_4$. Evaporation in rotary evaporator gave a crude solid (218 mg) which was dissolved in chloroform and purified by column chromatography (silica gel, chloroform/ethyl ether, 4:1). The yellow product was the only visible band, which after evaporation gave nitroxide **1**-OH as a yellow powder (147 mg, 59%). m.p. 191–193 °C. EPR (X-band): g = 2.0064, a_N = 14.6 G, spin concentration ≈ 100%. IR (cm^{-1}): 2934, 2921, ~2900 (broad, COO-H), 2874, 2853, 1719 (C=O), 1449, 1410, 1312, 1283, 1268, 1206, 1176, 1159, 1135, 907, 688, 671. HR FAB-MS (matrix: 3-NBA): 268.1915 (100%, $[M+2H]^+$ -0.9 ppm for $C_{15}H_{26}NO_3$), 267.1823 (9%, $[M+H]^+$ 4.2 ppm for $^{12}C_{15}{}^{1}H_{25}{}^{14}N^{16}O_3$), 266.1759 (17%, $[M]^+$ -1.0 ppm for $^{12}C_{15}{}^{1}H_{24}{}^{14}N^{16}O_3$).

Protocol for nitroxide **1**-NHS.

Run No.	SM (mg/mmol)	NHS (mg/mmol)	DCC (mg/mmol)	THF (mL)	Reaction time (h)	Yield (mg/%)	Spin Conc. (%)
1	123/0.462	41/0.356	98/0.475	4.0	67	314/90	
2	132/0.496	59/0.513	105/0.509	6.0	72		
3	91/0.342	54/0.469	94/0.456	5.8	45	99/80	
4	39/0.146	28/0.243	45/0.218	2.6	71	47/88	98
5	161/0.604	104/0.904	153/0.742	10.6	70	195/89	~100

Procedure based on run no. 5. Nitroxide radical **1**-OH (161 mg, 0.604 mmol), *N*-hydroxysuccinimide (NHS, 104 mg, 0.904 mmol), and *N*,*N*'-dicyclohexylcarbodiimide (DCC, 153 mg, 0.742 mmol) were charged to a 25 mL round bottom flask, briefly evacuated and filled with nitrogen. THF (10.6 mL, freshly distilled from sodium and benzophenone) was added and the resultant yellow solution was stirred at r.t. protected from light for three days. After eight hours a precipitate formed which remained through work up. After three days the reaction mixture was evaporated with a rotary evaporator and filtered through cotton with dichloromethane, evaporation of which yielded a crude solid (360 mg). The crude was dissolved in chloroform and purified by column chromatography (silica gel, chloroform/acetone, 97:3). The product was eluted first as a yellow band followed by an orange band of by-product. Evaporation of solvents yielded active ester **1**-NHS as a yellow-orange powder (195 mg, 89%). m.p. 182–184 °C. EPR (X-band) g = 2.0065, a_N = 14.6 G, spin concentration: ~100%. IR (ZnSe, cm^{-1}): 2930, 2858, 1809, 1782, 1737 (C=O), 1450, 1368, 1202, 1064, 1047, 993, 949, 908, 894, 813, 752, 736, 646. HR ESI-MS (MeOH/water, 3:1 and sodium acetate): 386.1814 ($[M+Na]^+$ 0.5 ppm for $C_{19}H_{27}N_2O_5Na$).

2.b EPR and ^{1}H NMR spectroscopic analyses of nitroxide radicals

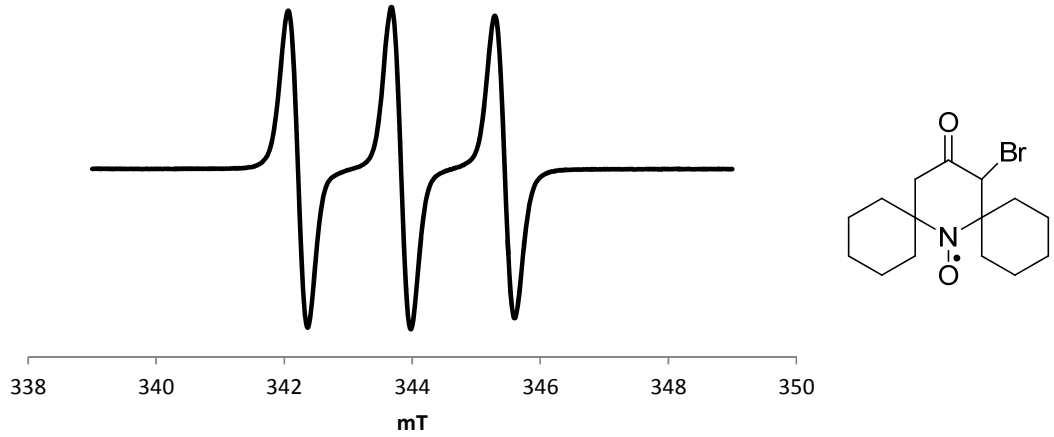

Fig. S1. EPR (X-band) spectrum of 1.0 mM **2**-Br in $CHCl_3$ for determination of spin concentration (sample label: jtp-3-100f1, EPR label: JP532r7).

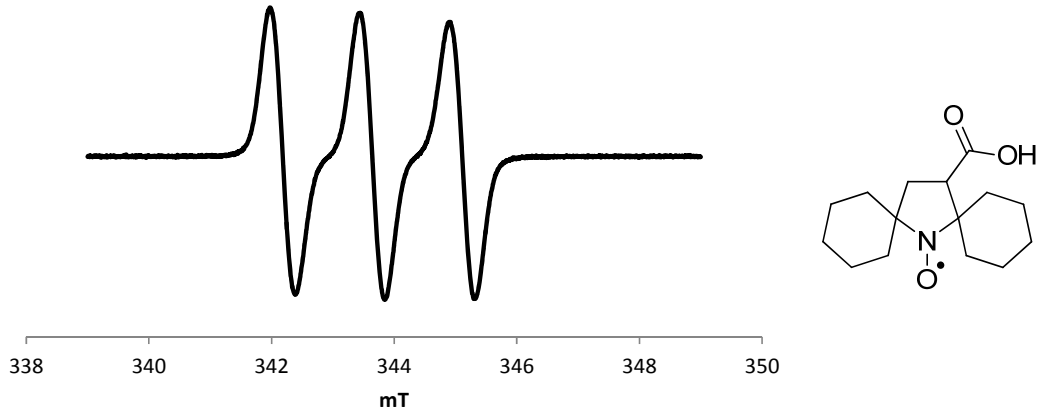

Fig. S2. EPR (X-band) spectrum of 1.1 mM nitroxide radical **1**-OH in $CHCl_3$ for determination of spin concentration (sample label: JTP-4-08f1, EPR label: JP528r12).

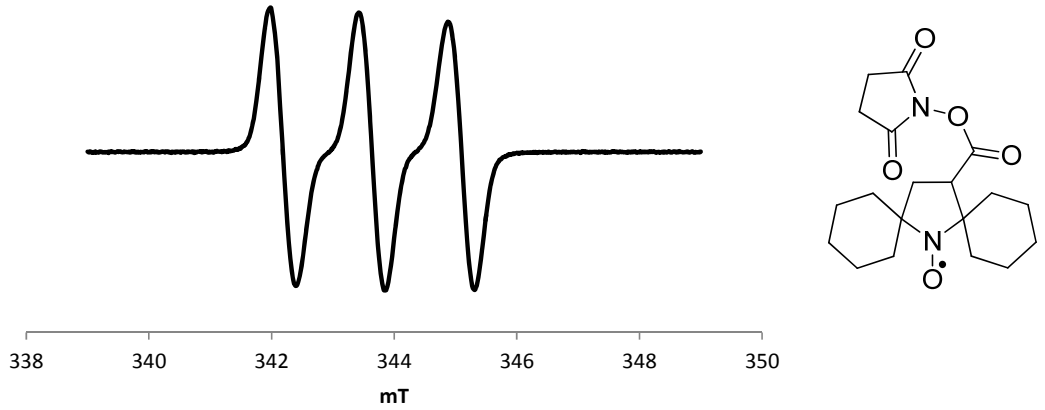

Fig. S3. EPR (X-band) spectrum of 1.0 mM nitroxide radical **1**-NHS in $CHCl_3$ for determination of spin concentration (sample label: JTP-3-41f1, EPR label: JP528r10).

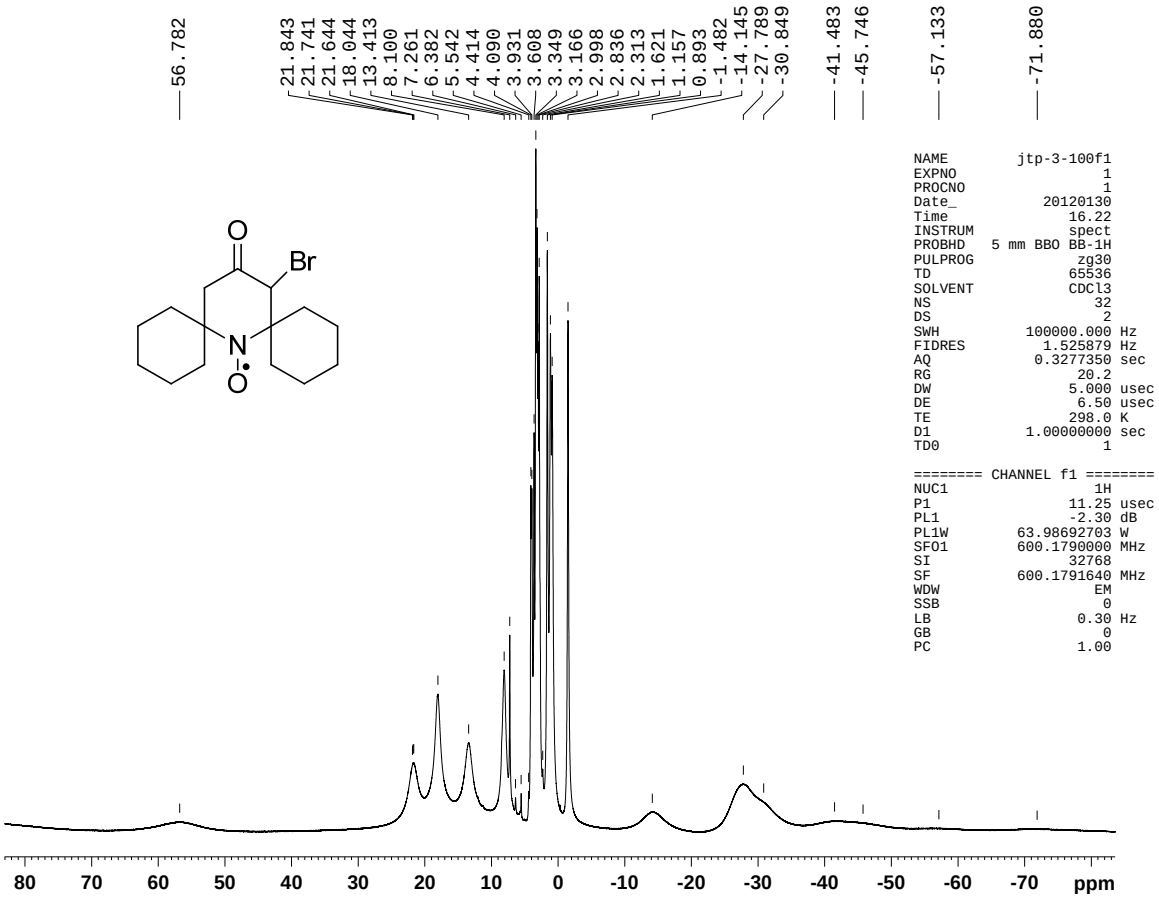

Fig. S4. ^{1}H NMR spectrum (600 MHz, $CDCl_3$) of bromo nitroxide **2**-Br (sample and NMR label: JTP-3-100f1).

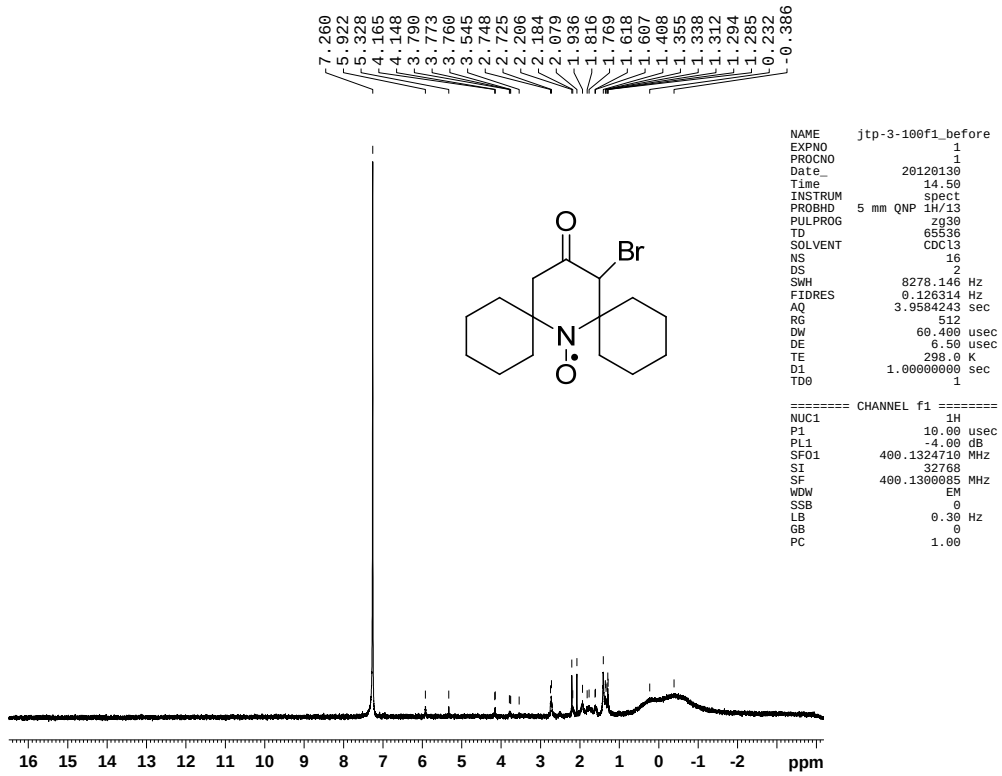

Fig. S5. ^{1}H NMR spectrum (400 MHz, $CDCl_3$) of dilute **2**-Br prior to reaction with phenylhydrazine (NMR label: JTP-3-100f1_before).

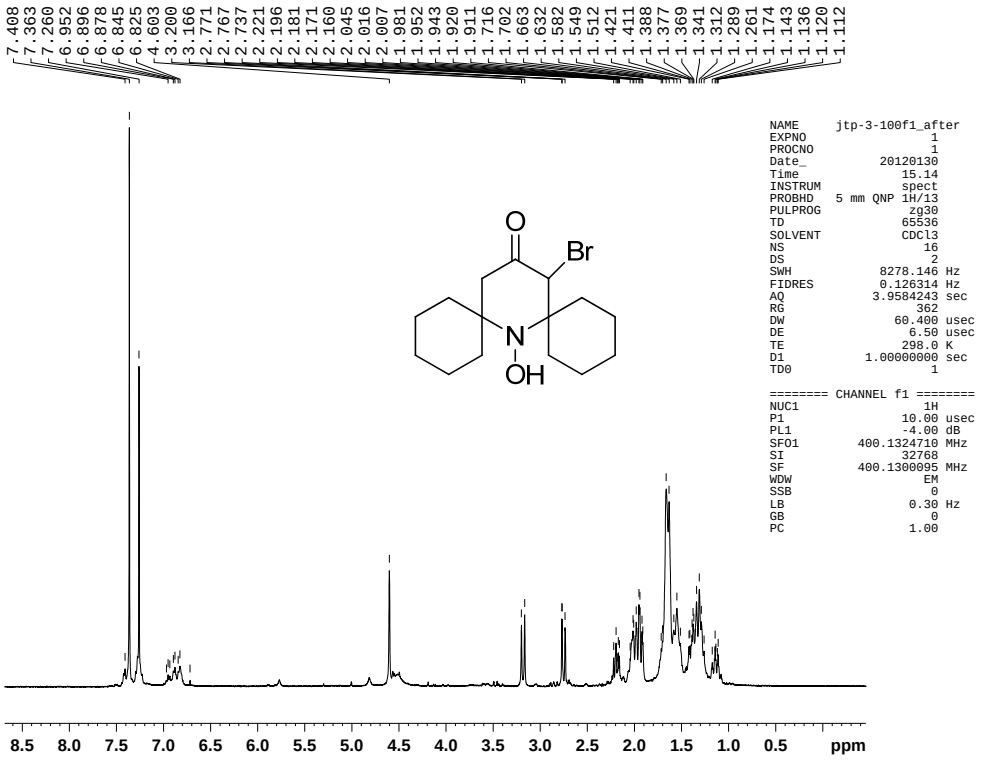

Fig. S6. ^{1}H NMR spectrum (400 MHz, $CDCl_3$) of the reaction mixture of **2**-Br with phenylhydrazine (NMR label: JTP-3-100f1_after).

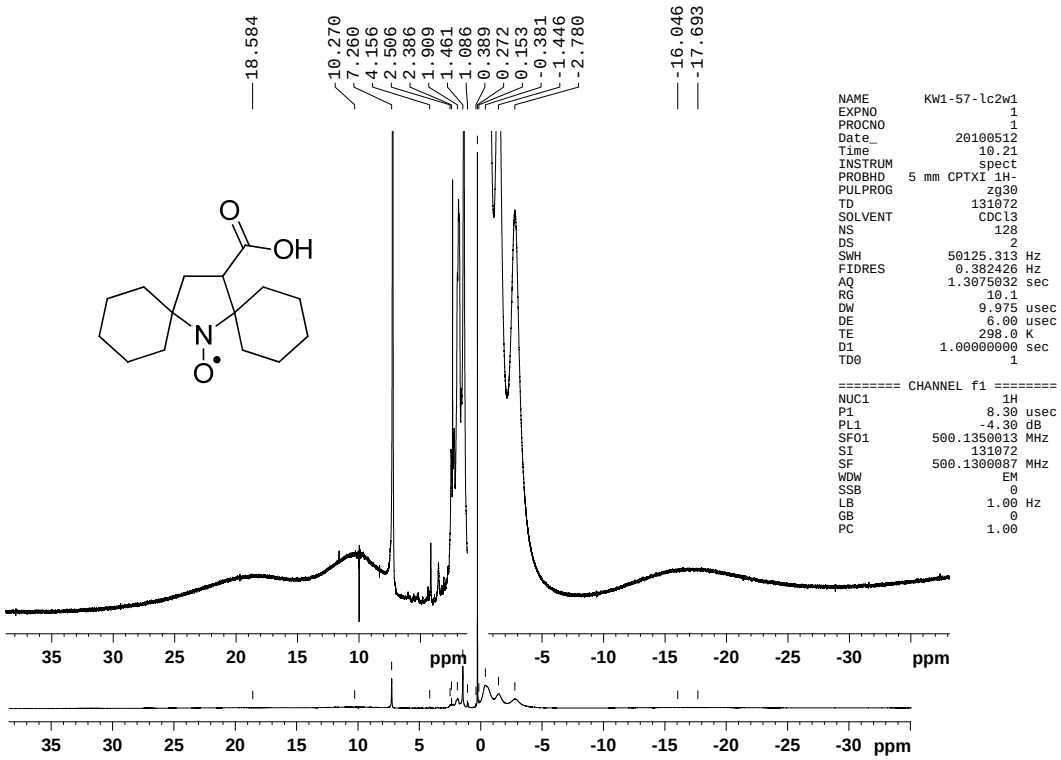

Fig. S7. ^{1}H NMR spectrum (400 MHz, $CDCl_3$) of nitroxide radical **1**-OH (sample label: KW1-57-lc2w).

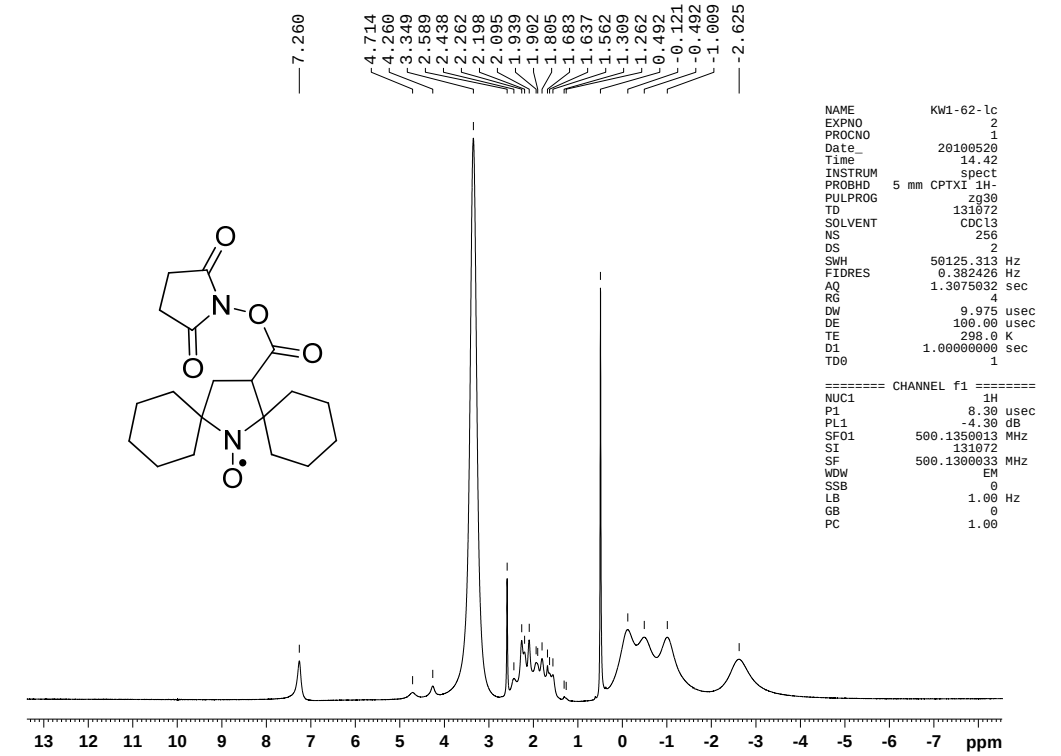

Fig. S8. ^{1}H NMR spectrum (400 MHz, $CDCl_3$) of nitroxide radical **1**-NHS (sample label: KW1-62-lc).

2.c Synthesis of organic radical contrast agents (ORCA).

Protocol for ORCAs based on **1**-mPEG-G4. PPI G4 dendrimer (33.6 mg, 4.70 μmol) and nitroxide radical **1**-NHS (36.2 mg, 99.7 μmol, 21 equiv, sample label: jtp0269f1) were weighed in a glovebag, and then dried under high vacuum for overnight. Then in the glovebag, a solution of PPI G4 dendrimer in anhydrous DMF (1.2 mL), and Hünig's base (60.0 μL, 73.5 equiv) were transferred to a Schlenk vessel. The Schlenk vessel was attached to high vacuum line, and then nitroxide radical **1**-NHS, as a solution in anhydrous DMF (0.4 mL) and anhydrous THF (0.4 mL), was added dropwise under inert gas flow (nitrogen or argon). The reaction mixture was lightly opaque during the addition of **1**-NHS, but turned into a clear light yellow solution after stirring for 20 min. After 6 days at room temperature in the absence of light, the homogenous reaction mixture was observed, though in some runs, a small amount of precipitate pasted on the wall of the Schlenk vessel was observed. Then to this solution, mPEG-12-NHS (174.8 mg, 267.2 μmol, 54 equiv) in anhydrous DMF (0.6 mL) was added. The reaction mixture was stirred at ambient temperature in the absence of light for another 6 days. The almost homogenous mixture with a small amount of suspended flocculent precipitate was centrifuged, and the precipitate was washed with DMF and centrifuged (×3). The combined clear DMF solutions were concentrated under dry nitrogen gas flow. Purification of the resultant clear pasty compound by dialysis (3500 D membrane) provided the product as yellow, clear, pasty solids with isolated yields of 81–97%. In this particular run, 151.4 mg (88%) of **1**-mPEG-G4 (sample label: yw0380B3) was obtained.

Table S1. Expanded version of Table 1 in the main text.

Sample label	ORCA	G	N	x (nitroxide equiv)	y (mPEG-12 equiv)	Spin Conc. (mmol g^{-1})	R_1 ($mM^{-1}s^{-1}$)[a]	τ_{rot} (ns)	*j* (radical)	*m* (mPEG)	*m/j*	Surface Coverage (%)
yw0380B3	**1**-mPEG-G4	4	64	21	54	0.41	0.450	1.4	12.6	35.8	2.84	75.6
									13.4	38.8	2.90	81.6
yw0380A3	**1**-mPEG-G4	4	64	21	54	0.40	-	-	12.4	36.0	2.90	75.3
yw0339C3	**1**-mPEG-G4	4	64	21	54	0.42	-	1.5	-	-	-	-
yw0509A4	**1**-mPEG-G4	4	64	22	64	0.41	0.419	1.6	13.6	40.3	2.96	84.2
									13.4	38.7	2.89	81.4
yw0488-5	**1**-mPEG-G4	4	64	22	65	0.42	0.401	-	-	-	-	-
yw0227-4	**1**-mPEG-G3	3	32	11	25	0.45	0.355	0.80	8	20	2.5	86
yw0425-3	**1**-mPEG-G3	3	32	11	25	0.46	0.385	0.88			-	-
yw0387-4	**1**-mPEG-G2	2	16	6	15	0.48	0.304	0.50	4	10	2.5	90
yw0427-3	**1**-mPEG-G2	2	16	6	15	0.43	0.282	0.47	-	-	-	-
yw0389cr2	**1**-mPEG-G0	0	4	1	5	0.23	0.211	0.25	-	-	-	-
yw0357-5	**1**-G4	4	64	70	0	2.38	-	-	42	-	0	65
yw0495-2	**1**-G4	4	64	80	0	2.34	-	-	40	-	0	63
yw0358-3	mPEG-G4	4	64	0	70	0	-	-	0	59	-	92
yw0233-5	3-CP-mPEG-G4	4	64	21	52	0.53	0.331	0.90	-	-	-	-
yw0419-3	3-CP-mPEG-G4	4	64	21	52	0.46	0.336	0.80	-	-	-	
3-Carboxy-Proxyl	3-CP	-	-	-	-	-	0.14	0.045	-	-	-	-

[a] R_1 ($mM^{-1}s^{-1}$) per S = ½ nitroxide radical.

Protocols for reduction of ORCA for the end group analysis by ^{1}H NMR spectroscopy.

Protocol based on the run with notebook label: yw03-99. A sample of **1**-mPEG-G4 (2.60 mg, spin concentration of 0.41 mmol/g, sample label: yw03-80B-3) was placed in a vial and dissolved in PBS buffer (0.15 mL, 71.6 mM, 10.1 equiv, prepared from equivalent amount of Na_2HPO_4 and NaH_2PO_4) in D_2O. Then, 0.14 mL of this solution of **1**-mPEG-G4 was transferred to 3-mm NMR tube, and then ascorbate (3.0 equiv, 20 μL of 150 mM solution in D_2O was added. The mixture was shaken to make a homogenous solution and kept at ambient temperature with exclusion of light for 15 h. ^{1}H NMR spectrum, obtained after the addition of 0.05 wt% 3-(trimethylsilyl) propionic-2,2,3,3-d_4 acid, sodium salt as the internal chemical shift standard (δ 0.00 ppm), suggested that the degree of reduction was sufficient for the end group analysis.

Purification of the reaction mixture by dialysis (3500 D membrane, 8 h in pure water) was followed by concentration, and then drying under high vacuum overnight, to provide a yellow pasty product corresponding to the reduced **1**-mPEG-G4 (1.92 mg, yield 74%, sample label: yw03-80B-3DR). This product was re-dissolved into 0.15 mL of pure D_2O and another ^1H NMR spectrum was obtained; end group analysis based on integration of ^1H NMR spectrum showed 35.8 mPEG-12 moieties per ORCA (Fig. S10, top spectrum).

Repeat run (notebook label: yw06-89) was carried out on the same sample of **1**-mPEG-G4 (sample label: yw03-80B-3) in PBS buffer (~85 μL of solution with spin concentration of 106 mM), which was recovered from *in vivo* MRI experiments (the sample amount is equivalent to 22.0 mg of neat sample with spin concentration of 0.41 mmol/g). Following the reaction with ascorbate, dialysis, concentration, and drying, the reduced **1**-mPEG-G4 (16.2 mg, yield: 73%, label: yw03-80B-3DR2B) was obtained as a light brown pasty solid. A 2.11 mg portion of the reduced product dissolved in D_2O to obtain ^1H NMR spectrum; end group analysis based on the integration of ^1H NMR spectrum showed 38.8 mPEG-12 moieties per ORCA (Fig. S10, bottom spectrum). The rest of the reduced product (13.7 mg) was dissolved in DMSO-d_6 to obtain ^1H NMR spectrum showing the two amide NH resonances at δ 7.9 and δ 10.4 ppm (see: main text and also Fig. S13 for a similar NMR spectrum on another sample). (Attempts to obtain ^1H-^1H COSY and ^1H-^{13}C HMBC spectra in DMSO-d_6 were not successful.) Subsequently DMSO-d_6 was removed (concentration, brief dialysis, concentration, and drying), to provide recovered product (11.41 mg (label: yw03-80B-3DR2C). This sample was then dissolved in 10% D_2O in H_2O, and another set of NMR spectra was obtained (Figs. S14 and S15).

This protocol is for a different sample of **1**-mPEG-G4; run with notebook label: yw05-23. Starting with **1**-mPEG-G4 (3.23 mg, spin concentration of 0.41 mmol/g, sample label: yw05-09A-4), the reduced **1**-mPEG-G4 (2.70 mg, yield: 84%, label: yw05-09A-4DR) was obtained as a light brown pasty solid. End group analysis based on integration of ^1H NMR spectrum showed 40.3 mPEG-12 moieties per ORCA (Fig. S11, top spectrum).

Repeat run (notebook label: yw06-96) was carried out on the same sample of **1**-mPEG-G4 (sample label: yw05-09A-4). Starting with **1**-mPEG-G4 (20.01 mg, spin concentration of 0.41 mmol/g, label: yw05-09A-4), the reduced **1**-mPEG-G4 (14.03 mg, yield: 70%, label: yw05-09A-4DR3) was obtained as a brown pasty solid. A 2.12-mg portion of the reduced product dissolved in D_2O to obtain ^1H NMR spectrum; end group analysis based on the integration of ^1H NMR spectrum showed 38.7 mPEG-12 moieties per ORCA (Fig. S11, bottom spectrum). Then in nitrogen gas filled glovebag, the rest of the compound (11.9 mg) was dissolved in 100%D DMSO-d_6 (0.14 mL), and then ^1H NMR spectra were obtained (Fig. S13). (In COSY and HMBC experiments, cross-peaks could not be observed, perhaps due to aggregation of **1**-mPEG-G4 in either DMSO-d_6 or DMSO-d_6/chloroform-*d* mixtures (e.g., 2:1, 0.2 mL).

Analogous protocols were used for reduction of **1**-mPEG-G3 and **1**-mPEG-G2; for ^1H NMR spectra in D_2O, see: Fig. S12.

The NMR spectroscopic samples used for the end group analyses of **1**-mPEG-G4, **1**-mPEG-G3 and **1**-mPEG-G2 showed EPR spectra with significantly decreased linewidth and intensity, indicating partial reduction of nitroxide radicals. Spin concentrations determined by EPR spectroscopy were in the 50–80% range of the values prior to the reduction and end group analysis.

End group analysis of ORCA: determination of number of nitroxide and mPEG-12 moieties. The number (m) of mPEG-12 moieties was calculated from ^{1}H NMR spectra of completely reduced ORCA in D_2O. The calculation is based on the ratio of the integral for the sharp singlet at δ 3.39 ppm (CH_3O group of mPEG-12) and half-peak integral of broad singlet at δ 1.91 ppm (CH_2 groups of the dendrimer core). For a sample of **1**-mPEG-G4, integral at δ 3.39 ppm was set to 3.00 protons and the integral at δ 1.91 ppm was found to be 3.46 protons, to give $m = (3.00/3)/2\times(3.46/248) = 35.8$.

Once the number m was determined, the number (j) of attached nitroxide moieties was calculated using spin concentration determined by EPR spectroscopy for ORCA in PBS buffer. The following relationship between spin concentration and the number j in **1**-mPEG-G4 was used:

$$\text{Spin Conc. (mmol/g)} = 1000\times j/[7167.8546 - (j+m)\times 1.0079 + j\times 249.3486 + m\times 571.6753]$$

In the above relationship, 7167.8546, 1.0079, 249.3486, and 571.6753 are molecular weights (g/mol) of the dendrimer core, hydrogen atom, nitroxide **1** moiety, and mPEG-12 moiety, respectively.

As illustrated in Fig. S9, for a sample of **1**-mPEG-G4 with $m = 35.8$ and spin concentration of 0.41 mmol/g, the value of $j = 12.6$ was found. Similar procedure was implemented for the end group analyses of **1**-mPEG-G3 and **1**-mPEG-G2, as well as for model compounds **1**-G4 and mPEG-G4.

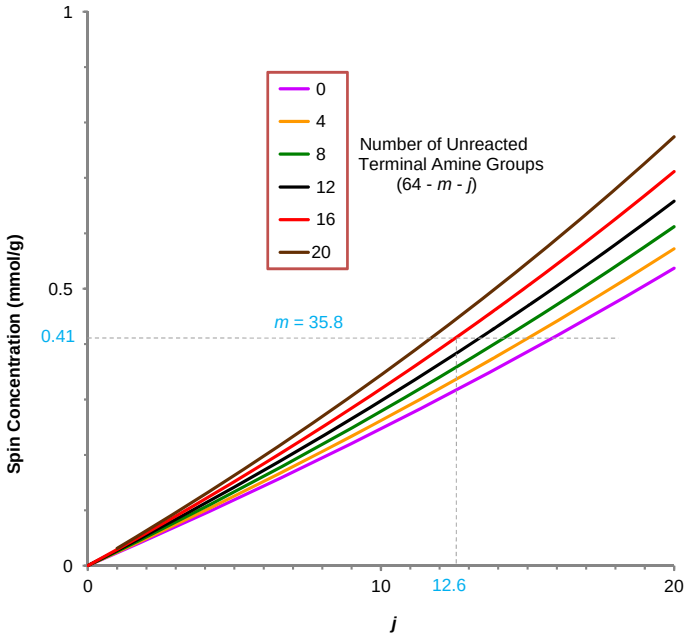

Fig. S9. Plot of spin concentration versus the number (j) of attached nitroxide moieties for selected numbers of unreacted terminal amine groups ($64 - m - j$) for ORCA **1**-mPEG-G4. For an example sample, the value of $j = 12.6$ is determined based on independently measured spin concentration (EPR) and value of m (^{1}H NMR) corresponding to the number of mPEG-12 moieties.

2.d NMR and IR spectroscopic analyses of ORCA after reduction with ascorbate.

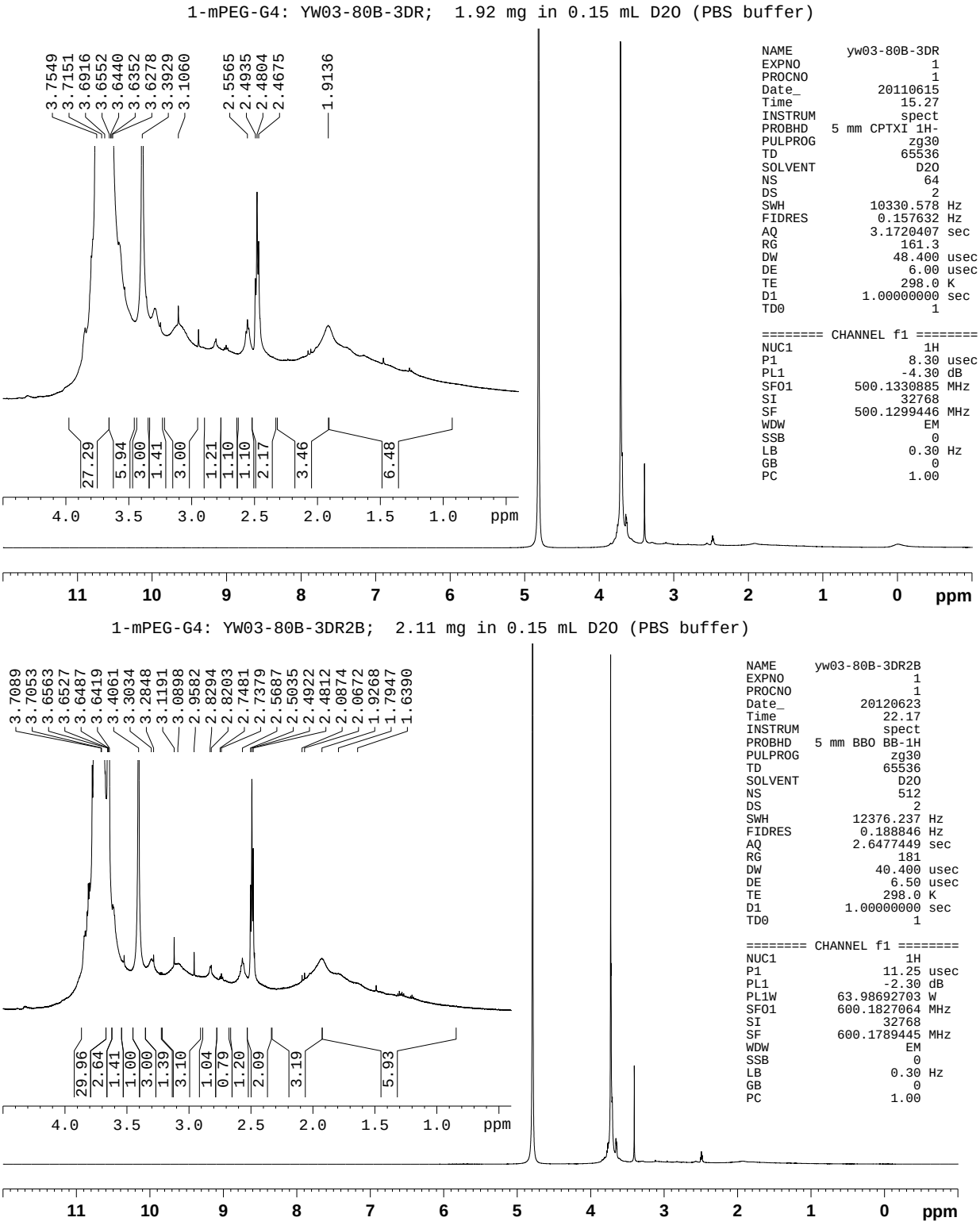

Fig. S10. ^{1}H NMR spectra (500 and 600 MHz, D_2O) of reduced **1**-mPEG-G4. Top and bottom spectra: two reduction runs on the same sample of **1**-mPEG-G4 (sample label: yw0380B3).

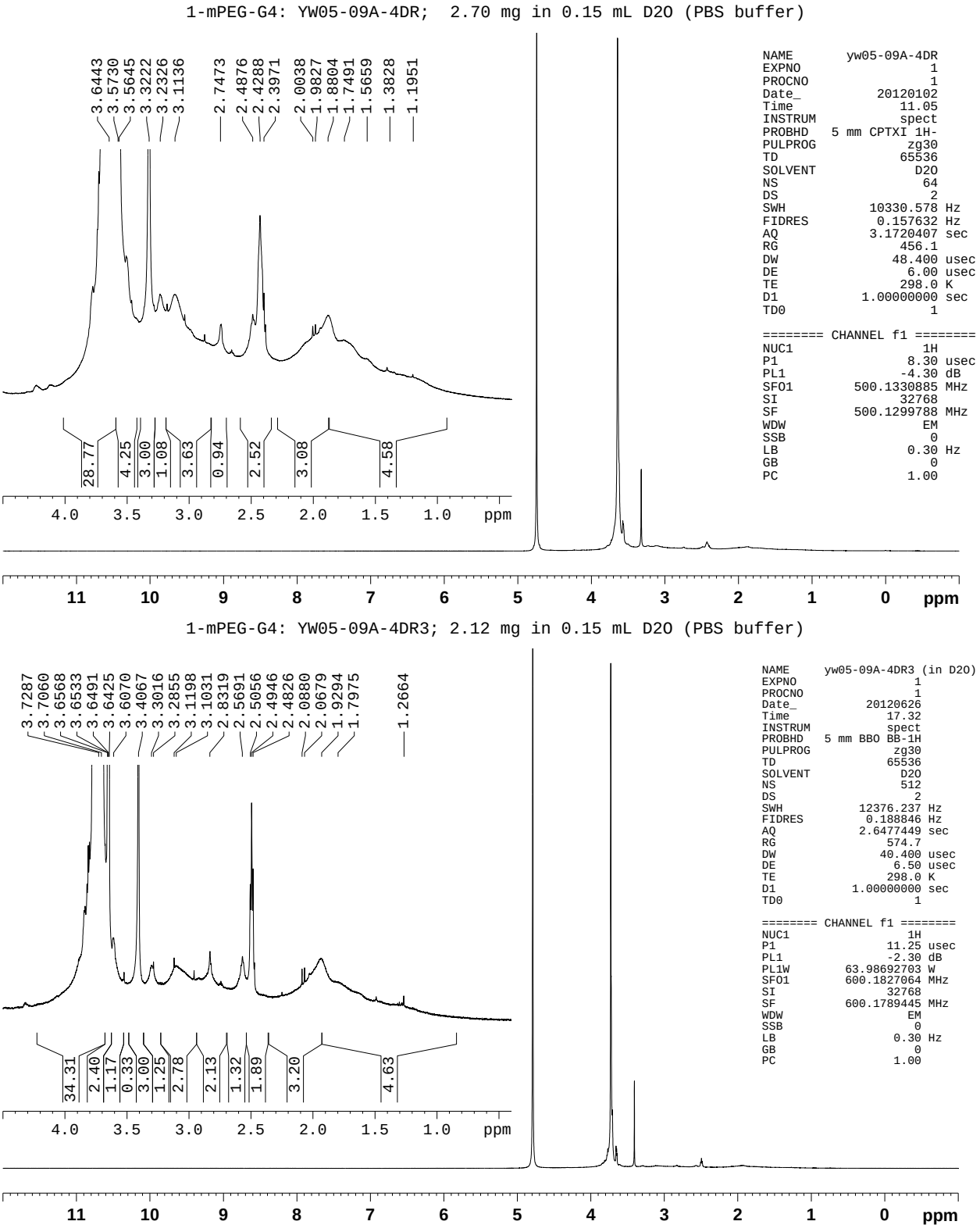

Fig. S11. ^{1}H NMR spectra (500 and 600 MHz, D_2O) of reduced **1**-mPEG-G4. Top and bottom spectra: two reduction runs on the same sample of **1**-mPEG-G4 (sample label: yw0509A4).

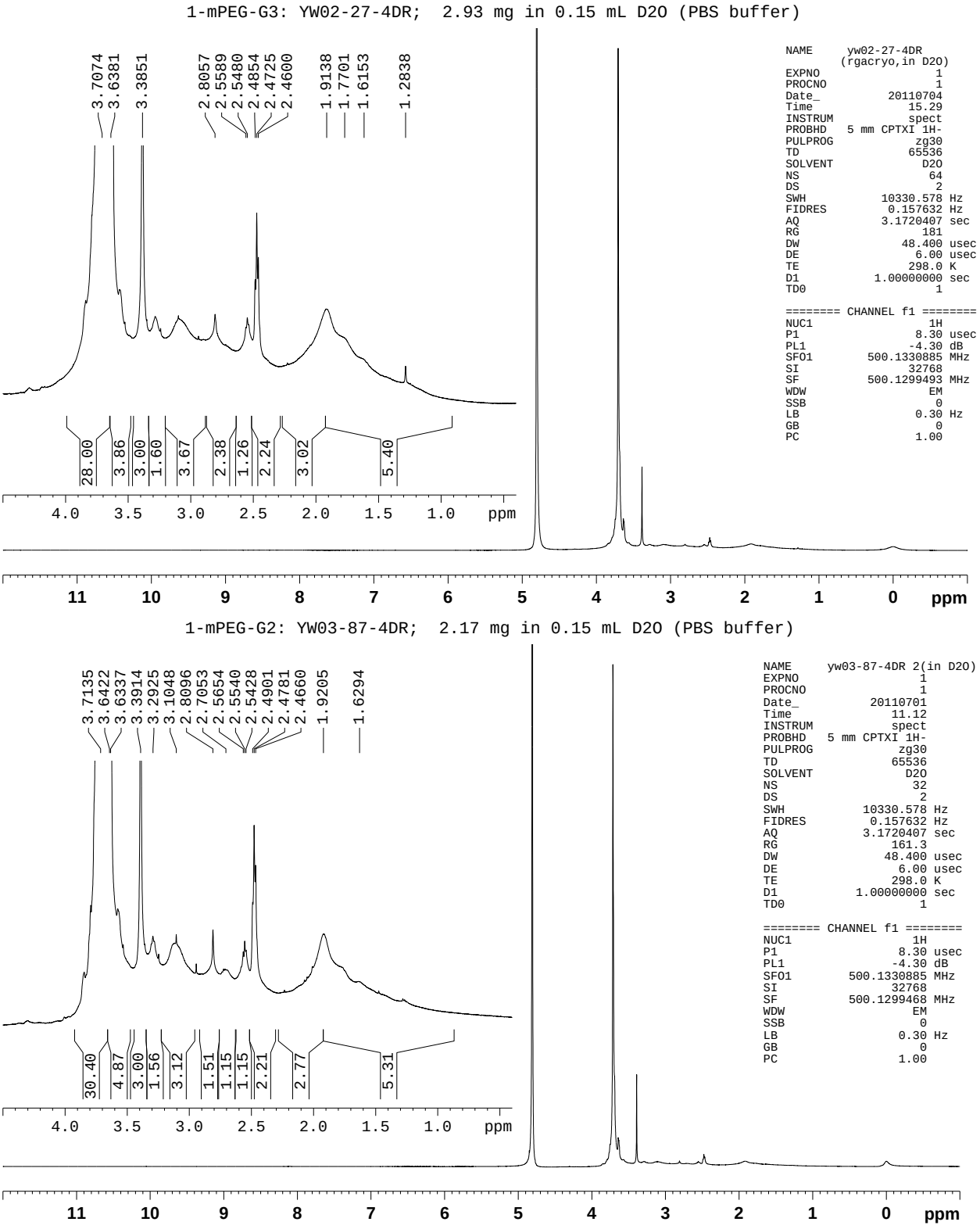

Fig. S12. ^{1}H NMR spectra (500 MHz, D_2O) of reduced **1**-mPEG-G3 (top spectrum) and **1**-mPEG-G2 (bottom spectrum) that were used for the end group analyses.

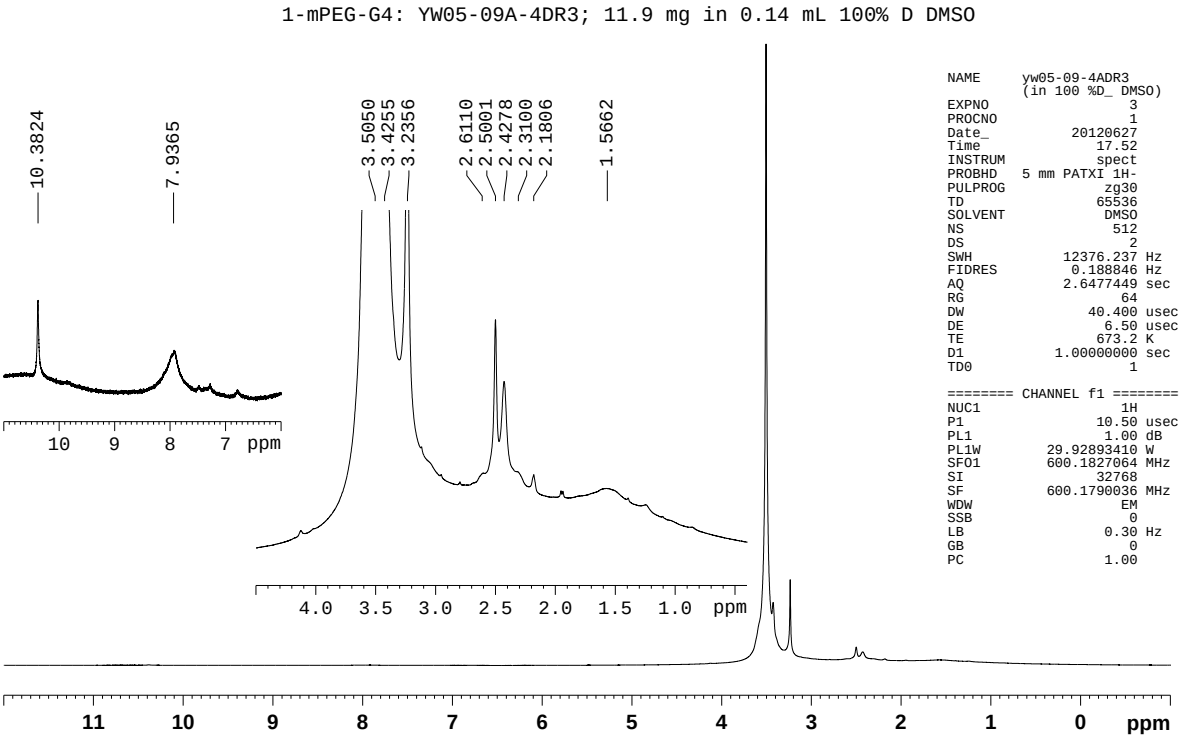

Fig. S13. ^{1}H NMR spectrum (600 MHz, DMSO-d_6) of reduced **1**-mPEG-G4 (sample label before reduction: yw0509A4). Peaks at δ 10.4 and δ 7.9 ppm were assigned to NH groups of the amide moieties connecting (reduced) nitroxides and mPEG-12 to the dendrimer core.

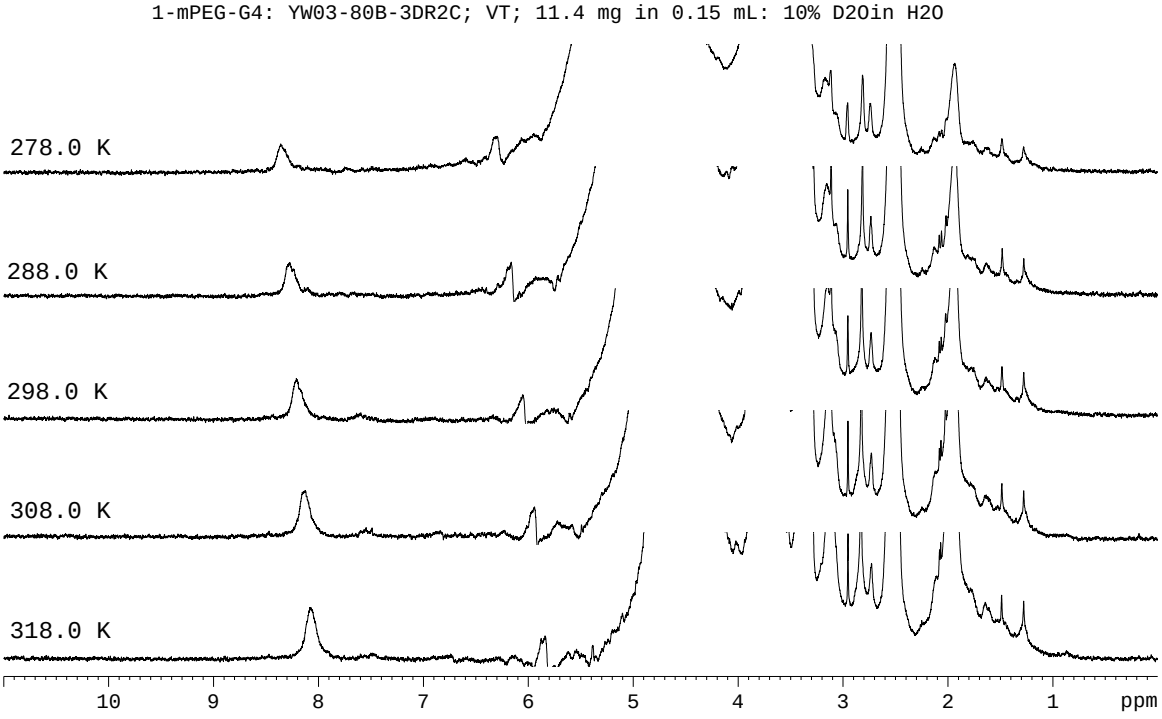

Fig. S14. ^{1}H NMR spectrum (600 MHz, 10% D_2O in H_2O) of reduced **1**-mPEG-G4 (sample label before reduction: yw0380B3). Peaks at δ 8.0 – 8.5 ppm were assigned to NH groups of the amide moieties.

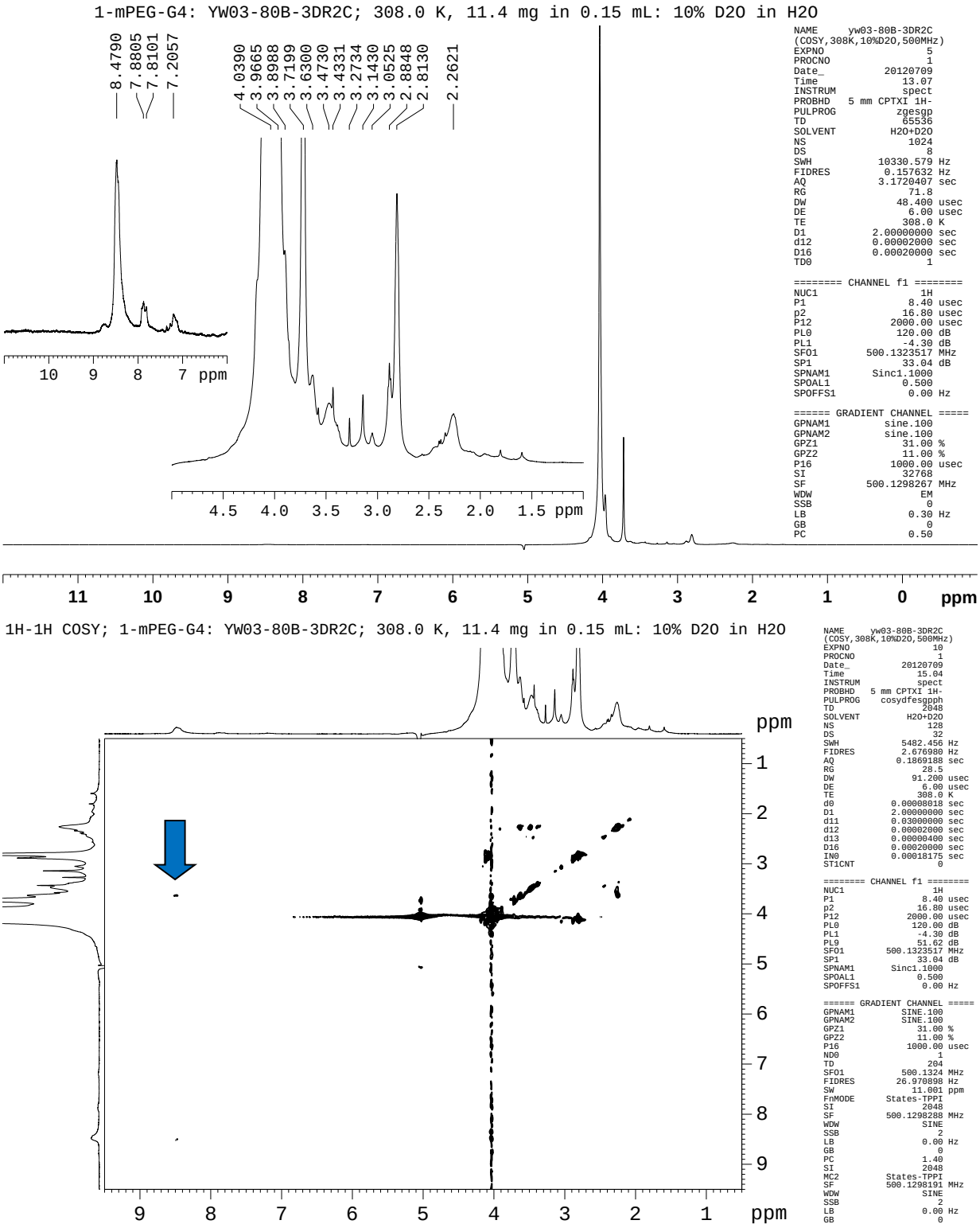

Fig. S15. ^{1}H NMR (top) and ^{1}H-^{1}H COSY (bottom) spectra (500 MHz, 10% D_2O in H_2O) of reduced **1**-mPEG-G4 at 308 K (sample label before reduction: yw0380B3). The cross-peak between the amide NH at δ 8.5 ppm and the NCH_2 of the dendrimer core at δ 3.6 ppm is labeled with a blue arrow.

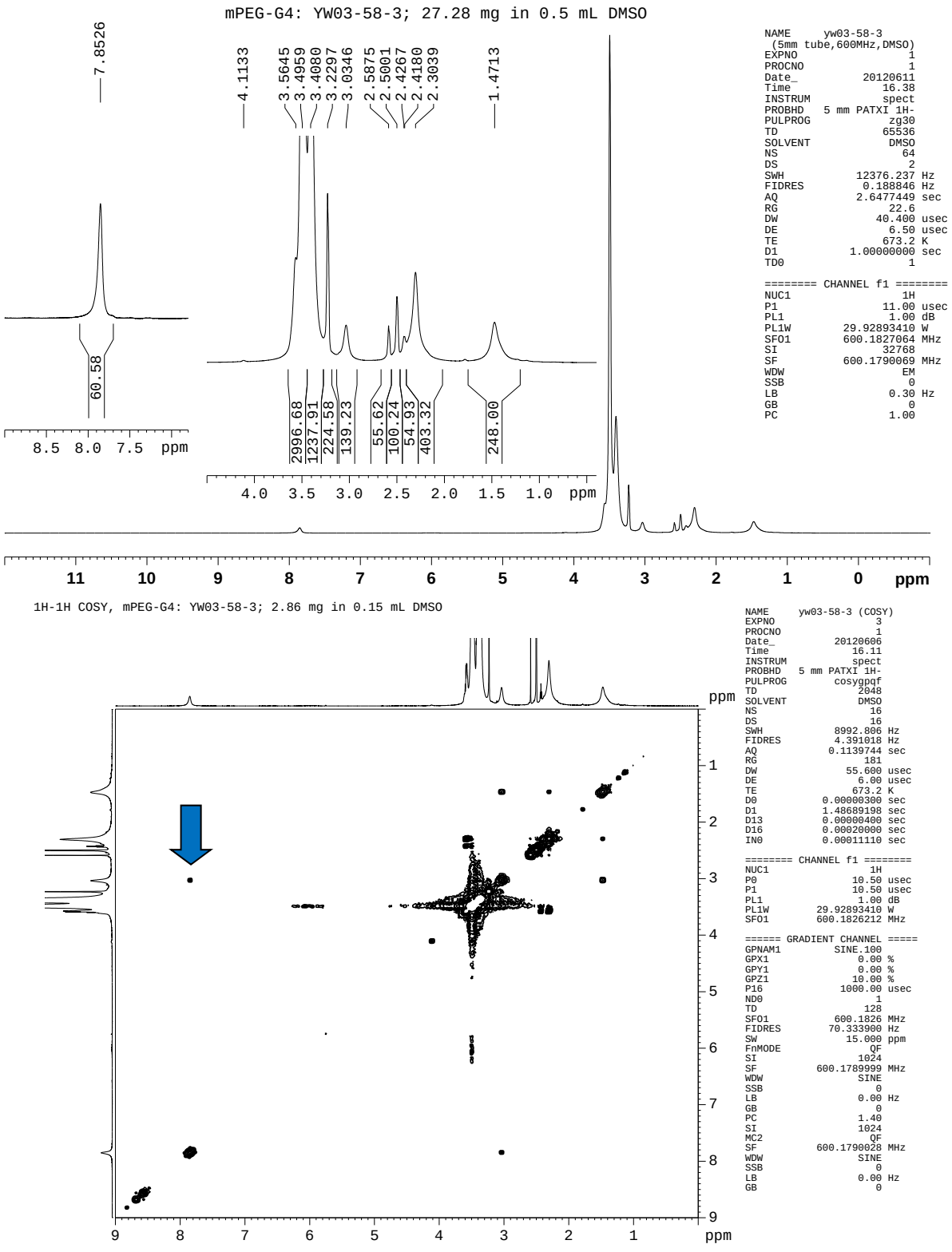

Fig. S16. ^{1}H NMR (top) and ^{1}H-^{1}H COSY (bottom) spectra (600 MHz, DMSO-d_6) of mPEG-G4 (sample label: yw03583). Peaks at δ 7.9 ppm and at δ 3.0 ppm, which have COSY cross-peak (see: blue arrow), were assigned to the NH groups of the amide moieties connecting mPEG-12 moieties to the dendrimer core and outermost NCH_2 of the dendrimer core.

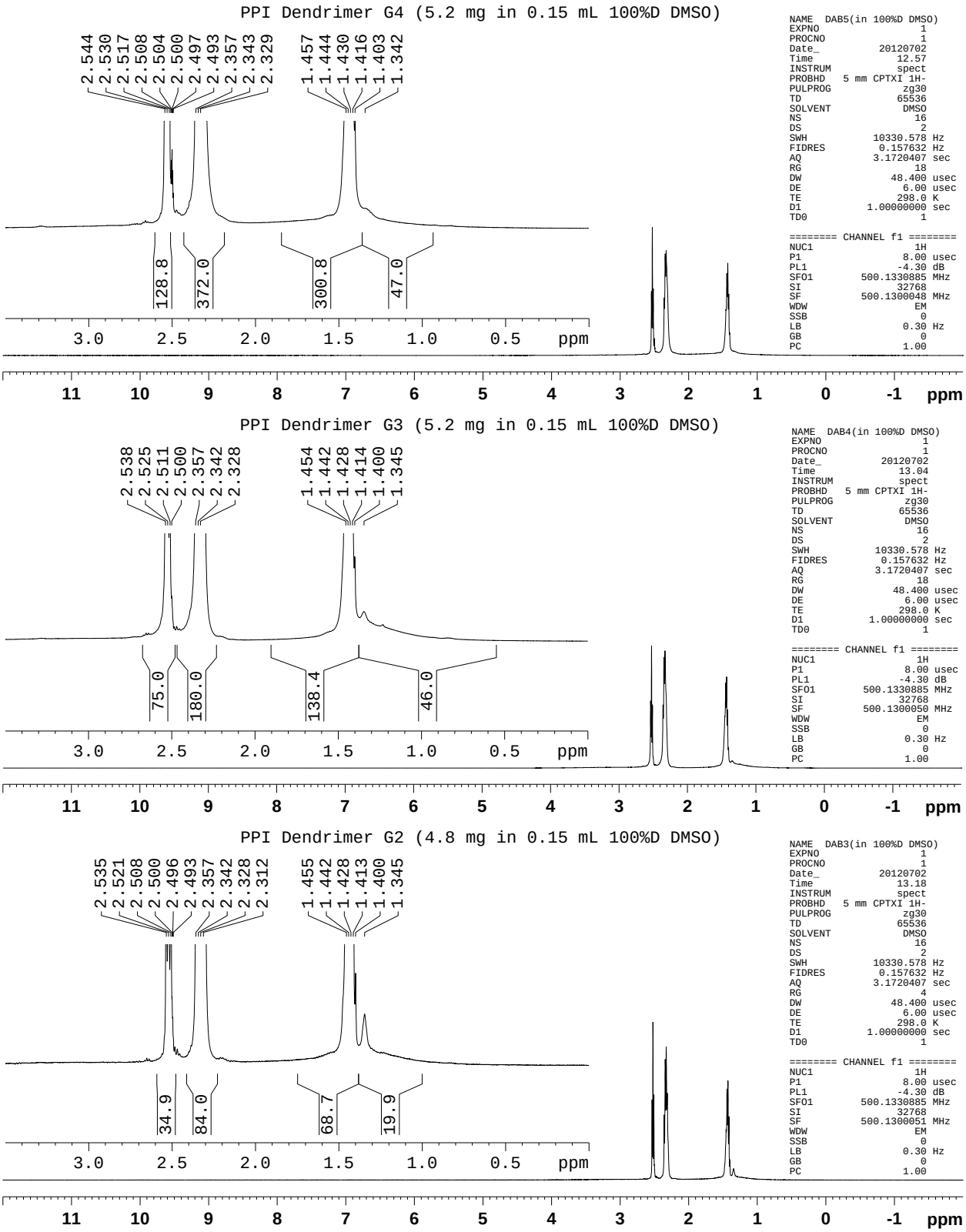

Fig. S17. ^{1}H NMR spectra (500 MHz, DMSO-d_6) of PPI dendrimers G4 (top plot), G3 (middle plot), and G2 (bottom plot). Peaks assigned to the terminal amine groups appear as broad singlet at approximately δ 1.5 ppm.

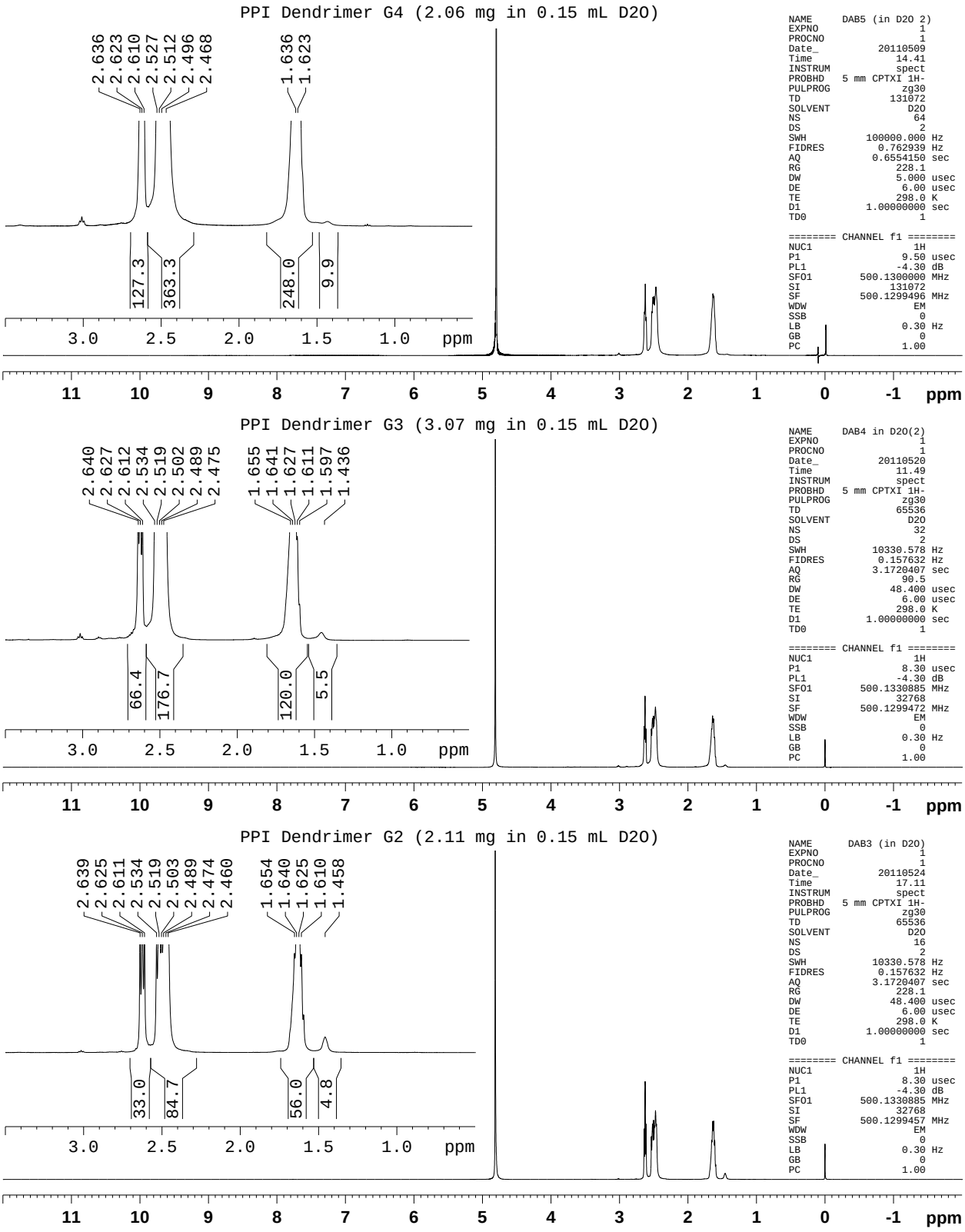

Fig. S18. ^{1}H NMR spectra (500 MHz, D_2O) of PPI dendrimers G4 (top plot), G3 (middle plot), and G2 (bottom plot).

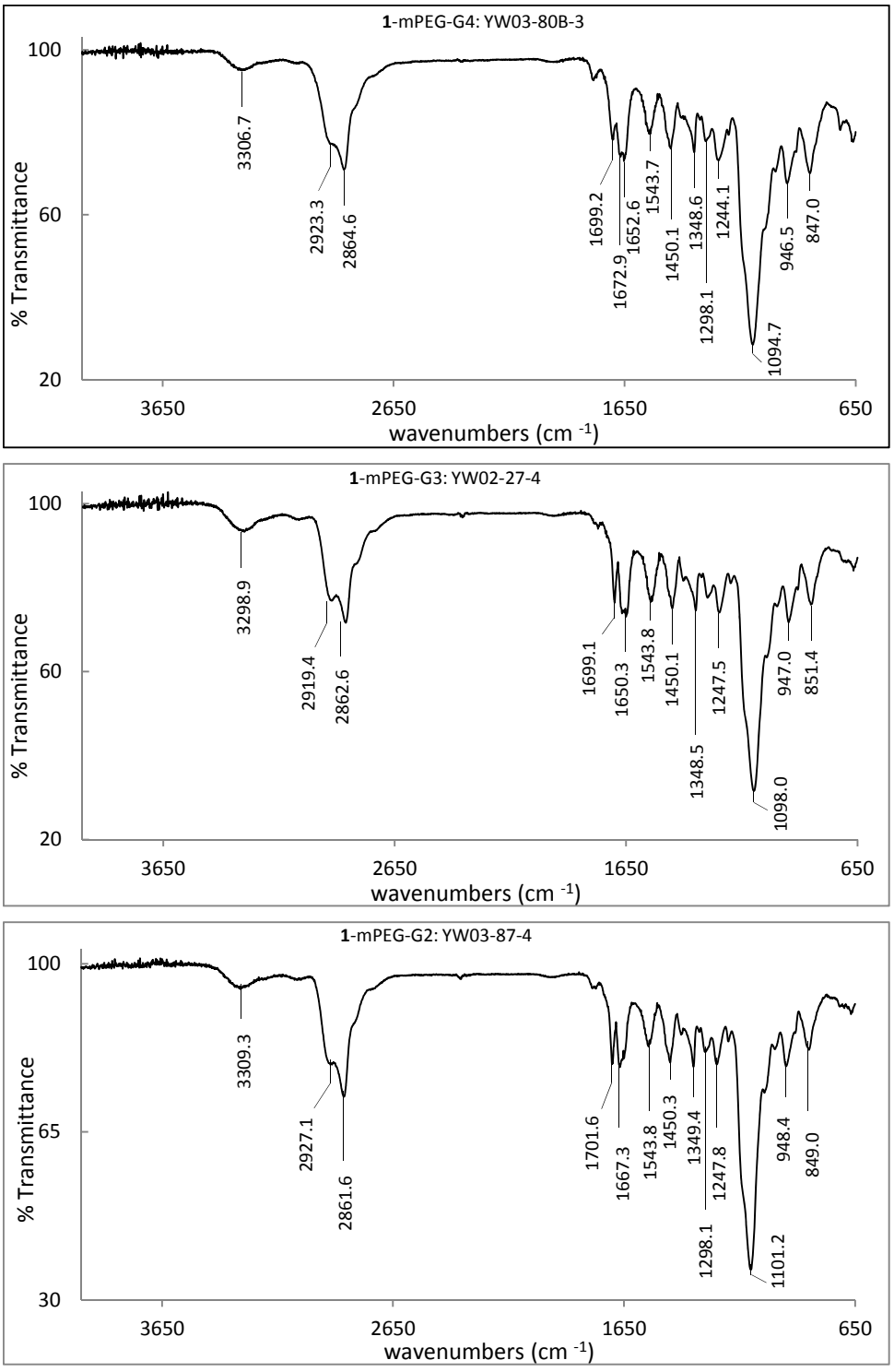

Fig. S19. IR (ZnSe, cm^{-1}) spectra for **1**-mPEG-G4 (top), -G3 (middle), and -G2 (bottom).

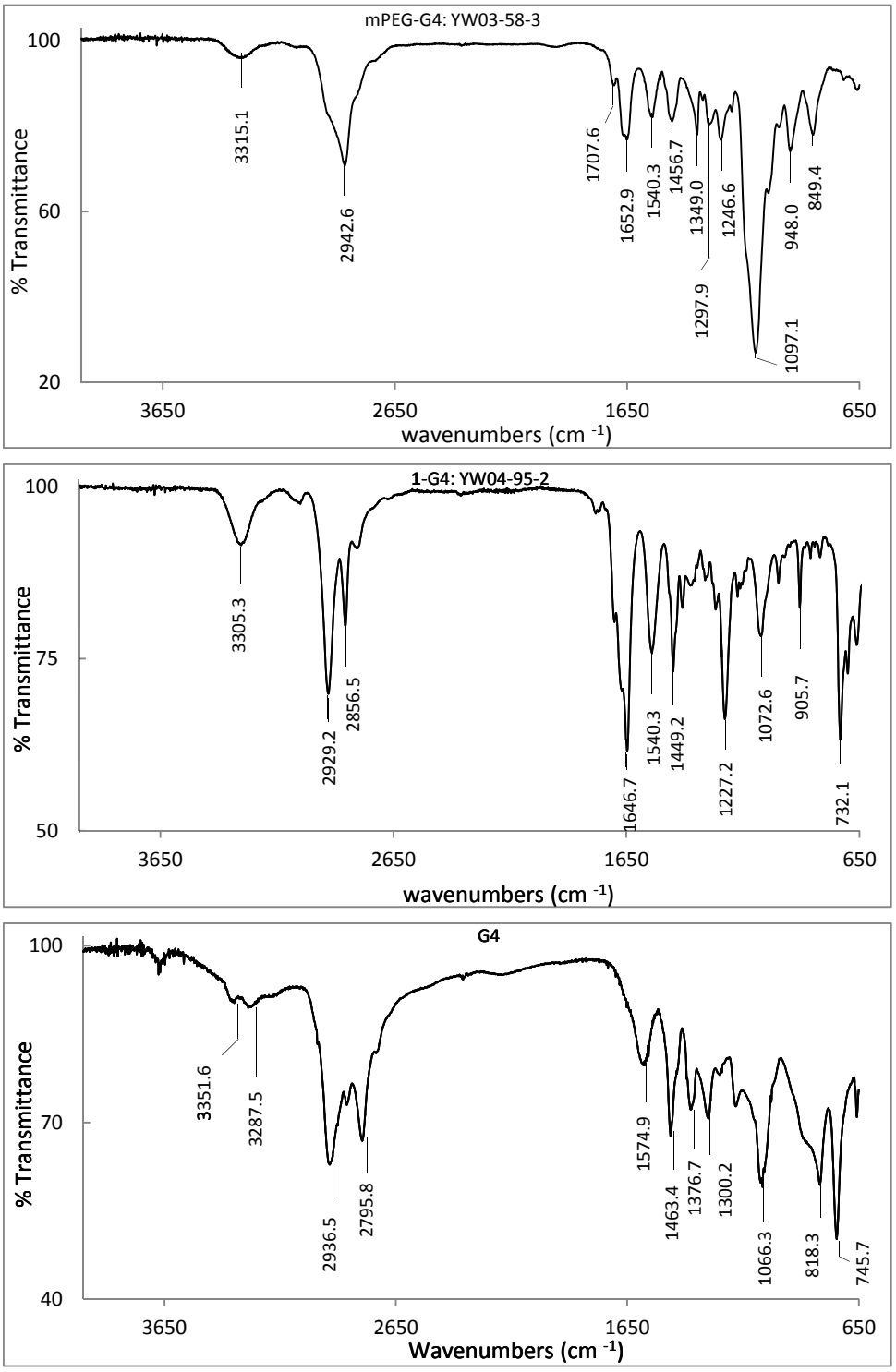

Fig. S20. IR (ZnSe, cm-1) spectra for mPEG-G4 (top), **1**-G4 (middle), and PPI-G4 dendrimer (bottom).

Section 3. *In Vitro* Characterization

3.a Kinetics of reduction of nitroxides with ascorbate. The results of kinetic measurements are summarized in Table S2 (this Section). The ascorbate solution was made with ascorbic acid, diethylenetriaminepentaacetic acid (DTPA, 0.1 mM), sodium hydroxide, and sodium phosphates (<30 ppm transition metals) at pH 7.4 (Corning pH/ion analyzer 350). Phosphate buffer was made with sodium phosphates and DTPA (0.1 mM) at pH 7.4 and used to make nitroxide solutions. Reactions were carried out with a 20 times molar excess of ascorbate[4].

Nitroxide and ascorbate solutions were combined in equal portions and mixed for 6 seconds. The resultant solution was drawn into an EPR-quality quartz capillary tube (I.D. 0.5 mm), and the capillary was stoppered with parafilm and placed in an EPR sample tube in the X-band spectrometer cavity. For low molecular weight nitroxide radicals, the peak height of the low-field line of the triplet was followed over time; the spectra were integrated to improve signal-to-noise as necessary. For high molecular weight nitroxides, i.e., ORCA, the peak height of the low-field peak of the non-integrated spectrum was followed; signal-to-noise was improved by using higher concentrations (Table S2). Microwave power was kept under 6.5 mW and temperature was controlled at 295 K with nitrogen flow system.

Table S2. Kinetics of nitroxide reduction with ascorbate under pseudo-first order conditions in PBS buffer with pH 7.4 at 295.0 K. Kinetic data are summarized for nitroxide 3-CP, nitroxide **1**, and ORCA **1**-mPEG-G4.

						Initial Kinetics (<1 h)				Late Stage Kinetics (after 1 h)		
Compd	Sample Label	Run No.	Run Label	Nitrox. Conc. (mM)	Asc. Conc. (mM)	k' $\times 10^4$ (s^{-1})	R^2	k ($M^{-1}s^{-1}$)	Avg k ($M^{-1}s^{-1}$)	k' $\times 10^4$ (s^{-1})	R^2	k ($M^{-1}s^{-1}$)
3-CP	-	1	JP460	0.20	4.00	2.547	0.9996	0.06368	0.063 ± 0.002			
3-CP	-	2	JP461	0.20	4.00	2.498	0.9975	0.06246				
3-CP	-	3	JP462	0.20	4.00	2.459	0.9999	0.06147		1.18	0.9952	0.030
1	jtp0408f1	1	JP480	0.20	4.00	1.262	0.9976	0.03155	0.031 ± 0.003			
1	jtp0408f1	2	JP481	0.20	4.00	1.142	0.9959	0.02854		0.708	0.9962	0.018
1	jtp0408f1	3	JP482	0.20	4.00	1.259	0.9991	0.03147				
1-mPEG-G4	yw0380B3	1	JP609	0.50	10.0	6.196	0.9810	0.06196	0.058 ± 0.004	0.29	0.9874	0.0029
1-mPEG-G4	yw0380B3	2	JP610	0.50	10.0	5.420	0.9766	0.05420				
1-mPEG-G4	yw0380B3	3	JP611	0.50	10.0	5.725	0.9985	0.05725				

3.b Relaxivity (r_1) and stability of ORCA. The results of relaxivity (r_1) measurements are summarized in Table S1 (Section 2).

Relaxivity of ORCA. Prior to relaxivity measurements, stock solutions of 3-CP, **1**-mPEG-G4, **1**-mPEG-G3, **1**-mPEG-G2, **1**-mPEG-G0, and 3-CP-mPEG-G4 in PBS pH 7.2 were examined by EPR spectroscopy to determine spin concentrations. Then, each stock solution was serially diluted with PBS pH 7.2 to provide 0.1-mL samples in 0.2-mL polypropylene centrifuge tubes, which were placed in a phantom holder. MRI data were obtained using a 7 Tesla/16 cm scanner (Bruker Pharmascan) at room temperature.

Stability of ORCA. A stock solution of **1**-mPEG-G4 (sample label: yw0509A4, spin conc. = 0.41 mmol/g) in PBS, pH 7.2 was determined to have spin concentration of 8.4 mM by EPR spectroscopy (EPR label: AO-8-25). Serial dilution of the stock solution was followed by phantom relaxivity study, which showed no significant decrease of r_1 over 29 h at room temperature (Fig. S21).

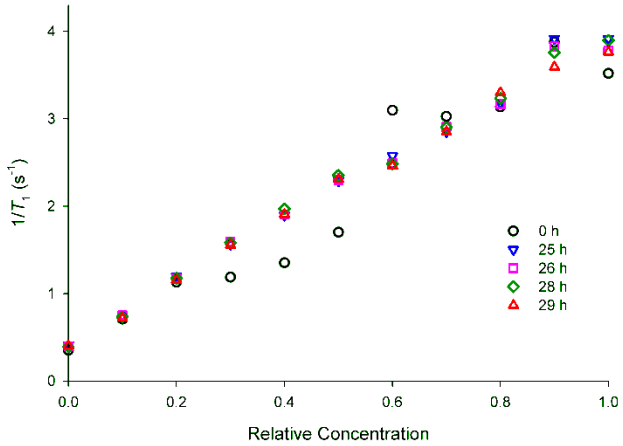

Fig. S21. Plots of water ^{1}H relaxation rates, $1/T_1$, vs. relative concentration of nitroxide radicals in **1**-mPEG-G4 in PBS pH 7.2 after indicated period of time at room temperature. Concentration range, determined by EPR spin concentration, 0 – 8.4 mM; magnetic field strength of 7 Tesla.

A sample **1**-mPEG-G4 (sample label: yw0380B3) in PBS (6.7 mM, pH 7.4), recovered after *in vivo* experiments, was determined to possess a spin concentration of 99 mM by EPR spectroscopy (reference: 3-CP)(EPR label: jtp-4-07). After storing the sample for 5 months in a –20 °C freezer, the spin concentration was 106 mM, i.e., unchanged within experimental error (EPR label: yw0689).

3.c Rotational correlation times (τ_{rot}), electron spin relaxation times (T_{1e} and T_{2e}), and factors limiting R_1.

Rotational correlation times. Spin-labeled dendrimers were suspended in PBS buffer (pH 7.4) and reduced using a 3:1 molar ratio of ascorbic acid to spin label. Reduction was needed to decrease the local nitroxyl concentration which causes significant exchange broadening of the CW EPR lineshape. Spin label concentration was determined by comparison of CW EPR integrals with a nitroxyl standard. Samples were reduced until the spin labeled concentration was approximately 100 μM before spectra were recorded for simulation. Room temperature CW EPR spectra were recorded on a Bruker EMX spectrometer at 9.8 GHz (X-band) using 2 mW microwave power, 1 G modulation amplitude at 100 kHz, 1.28 ms time constant and 40.96 ms conversion time. Between 5 and 25, 100 G scans were averaged depending on the concentration and extent of reduction of each sample. Tumbling correlation times (τ_{rot}) of the spin-labeled dendrimers were calculated by simulation of the CW EPR lineshapes using the *chili* toolbox of EasySpin[5]. Linewidths of the center lines were manually adjusted and then held constant as the τ_{rot} was varied to give the best fit to the low-field and high-field lines. The results of rotational correlation times (τ_{rot}) measurements are summarized in Table S1 (Section 2) and Figs. S23 and S24 in this Section.

Electron spin relaxation times (T_{1e} and T_{2e}). In the tumbling ranges for these ORCA T_{1e} is expected to be substantially longer than T_{2e}, but that difference may be decreased by the electron-electron spin exchange. The lineshapes for the EPR spectra of the spin-labeled dendrimers are not simple Lorentzians, which is attributed to a distribution of environments for the labels and unresolved hyperfine splittings. When the lineshapes for **1**-mPEG-Gn (n = 4, 3, 2) were approximated as Lorentzians, the linewidths ranged from 3.5 to 4 G, which corresponds to

T_{2e} of 19 and 16 ns. The constraint $T_{1e} > T_{2e}$ then requires that T_{1e} for these ORCA is longer than about 20 ns.

Factors limiting r_1. Analyses using equations S1–S4 (Fig. S22A), which are adopted as standard in the analysis of Gd-chelates, suggest that per-nitroxide r_1 may be increased to values significantly greater than 0.4 $mM^{-1}s^{-1}$. Similar to the gadolinium chelates, nitroxide radicals form complexes with at least one water molecule[6]. According to eq. S1, longitudinal ^1H water relaxivity (r_1), i.e., per-nitroxide r_1, is the sum of inner-sphere and outer-sphere contributions. The inner-sphere contribution is dominant, and thus by far the most important for optimization[7]. For nitroxide radicals, the primary inner sphere relaxation mechanism is the dipolar relaxation[7,8]. The same relaxation mechanism is expected in ORCAs, which may be considered as ensembles of weakly coupled, independent $S = ½$ radicals, analogous to $S = 7/2$ gadolinium chelates attached to dendrimers. The dipolar inner sphere relaxivity (r_{1inner}) of water (55.55 M) per $S = ½$ nitroxide is governed by standard equations S2, S3, and S4 (Fig. S22A)[7,9].

Equations S2-S4 may be used to obtain plots of r_{1inner} vs. τ_{exch} for selected values of τ_{rot} or T_{1e} (Fig. S22B and S22C). These plots of r_{1inner}, which is expected to be the dominant contributor to r_1,[7] suggest that in order to account for the measured values of $r_1 \approx 0.40$ $s^{-1}mM^{-1}$ observed for **1**-mPEG-G4, τ_{exch} has to be quite long, i.e., $\tau_{exch} \approx 50$ μs (very slow rate $1/\tau_{exch}$). Calculations of r_{1inner} also illustrate a potential, as well as limits, in optimization of r_1. For example, if water exchange rate ($1/\tau_{exch}$) can be increased so τ_{exch} is shortened to about 1 μs, a typical value for per-nitroxide, $r_1 \approx 5$ $s^{-1}mM^{-1}$ is possible for an ORCA with $\tau_{rot} \approx 1.5$ ns and $T_{1e} \approx 20$ ns.

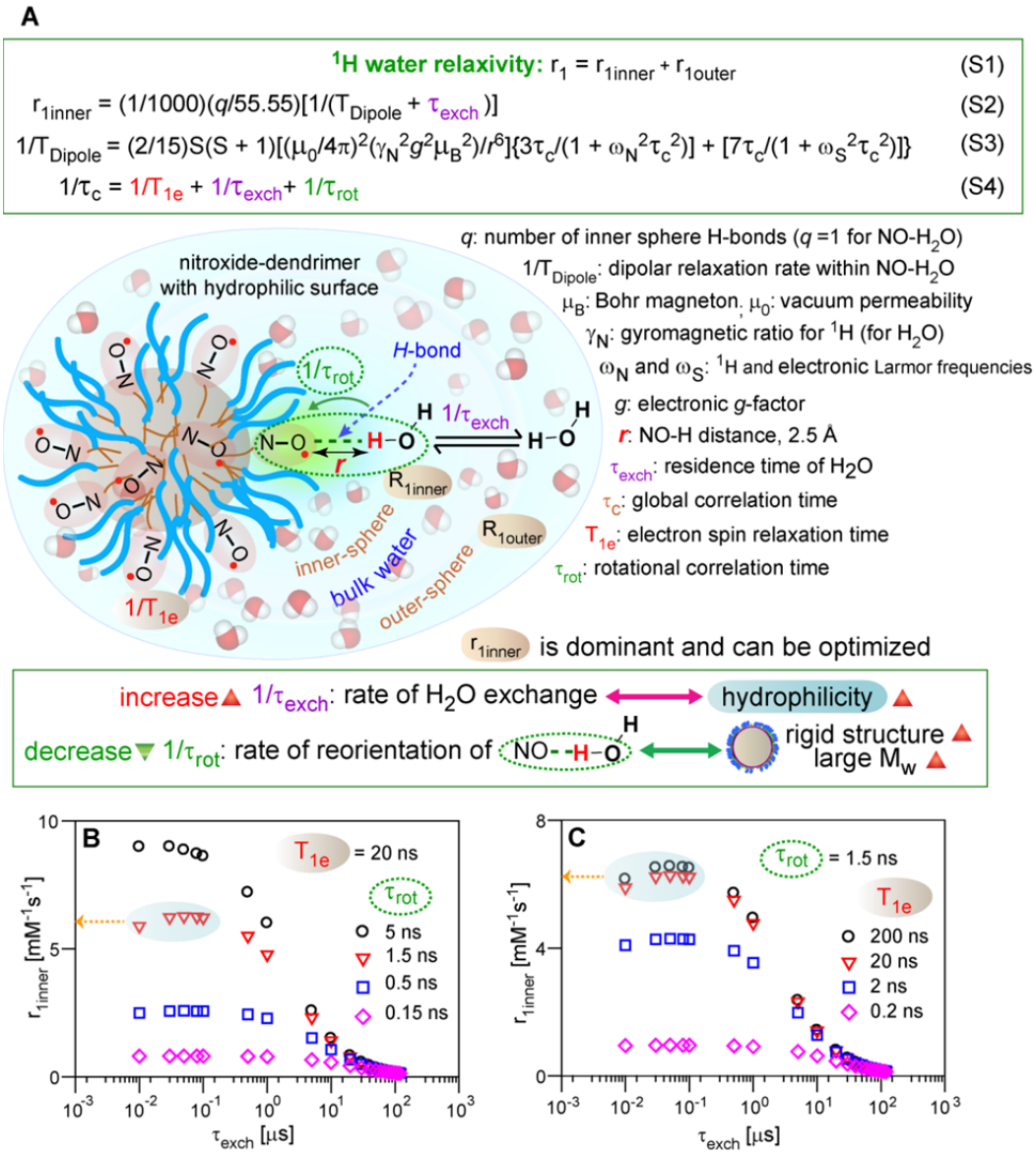

Fig. S22. Factors limiting r_1. (**A**) Dipolar inner sphere model for water ^{1}H relaxivity r_1 per S = ½ nitroxide radical. (**B**) and (**C**) Plots of dipolar inner sphere relaxivity (r_{1inner}) per S = ½ nitroxide radical versus residence time of water (τ_{exch}) for selected values of T_{1e} and τ_{rot}.

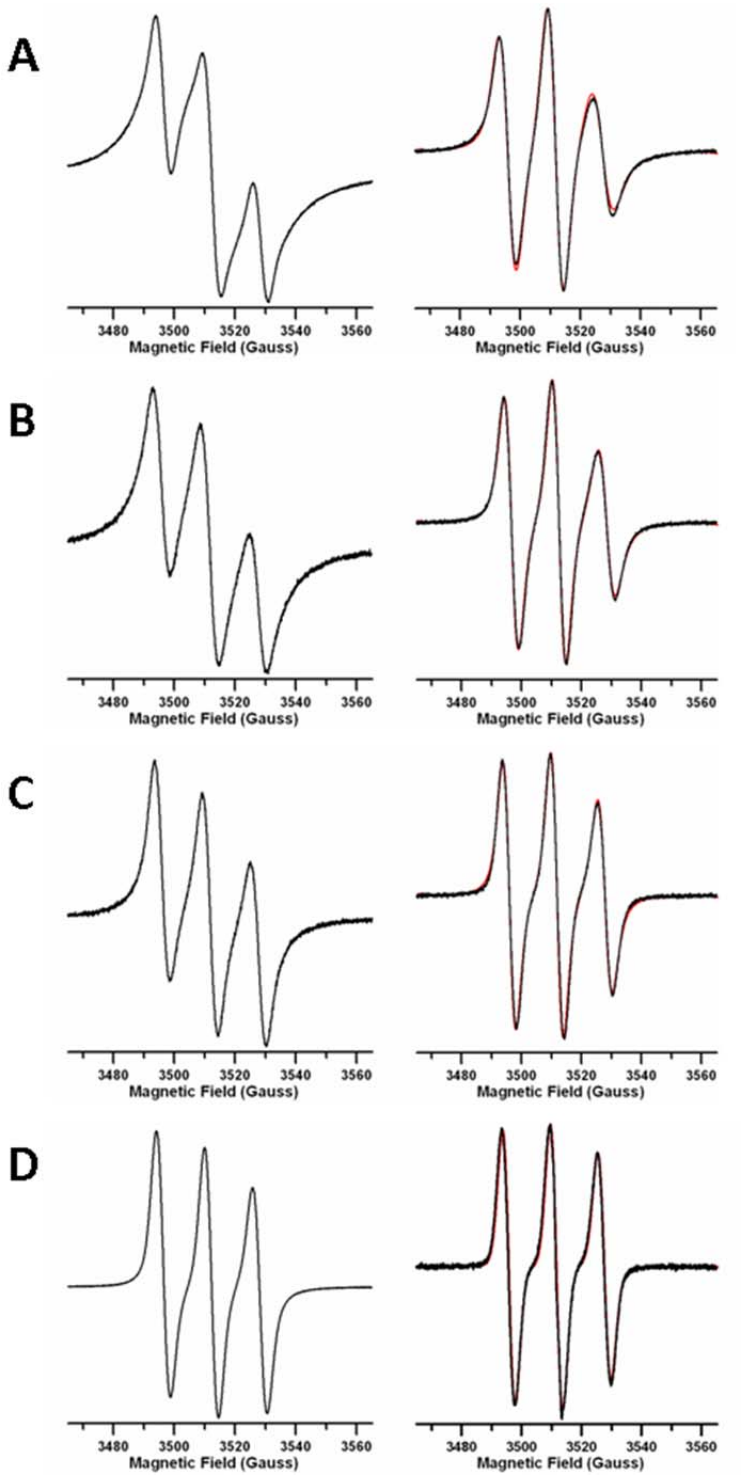

Fig. S23. CW EPR spectra of **1**-mPEG-G4 (A), -G3 (B), -G2 (C) and -G0 (D) PPI dendrimers before (left) and after (right) reduction. For reduced spectra, data (black) and EasySpin simulations (red) are shown.

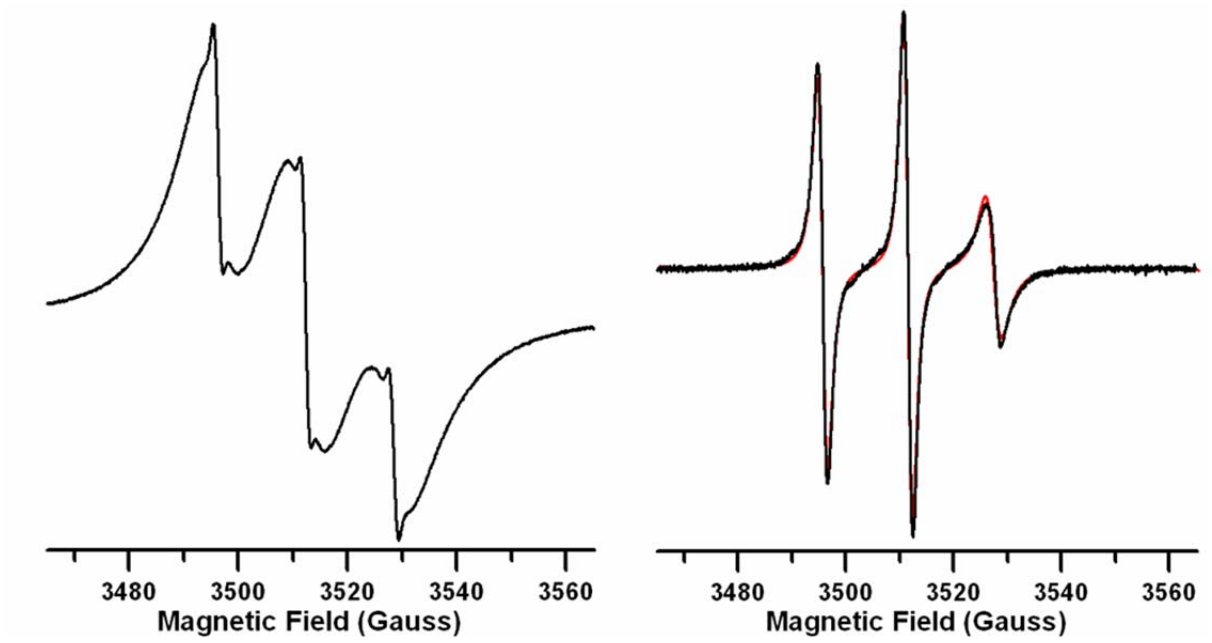

Fig. S24. CW EPR spectra of 3-CP-mPEG-G4 PPI dendrimers before (left) and after (right) reduction. For reduced spectrum, data (black) and EasySpin simulations (red) are shown.

Section 4. *In Vivo* Characterization

*ORCA **1**-mPEG-G4.* Solutions of **1**-mPEG-G4 were prepared in physiological PBS, to obtain 120 mM spin concentration of $S = ½$ nitroxide radicals. Volume of the injected solution was 110 μL, corresponding to a dose of ~13 μmol of $S = ½$ nitroxide radicals per mouse. Following the injections, spin concentration of each stock solution was verified by EPR spectroscopy.

Mice. MRI was performed on C57 Bl6 mice in this study in accordance with protocols approved by the Institutional Animal Care and Use Committee at the University of Nebraska Medical Center (UNMC). Animals were obtained from the Jackson Laboratories (Bar Harbor, ME) and housed under specific pathogen-free conditions in accordance with the ethical guidelines for care of laboratory animals at UNMC and set forth by the National Institutes of Health.

MRI acquisition. Mice were anesthetized by inhalation of 1–2% isoflurane in a nitrous oxide/oxygen mixture before and during MRI data acquisition. Before MRI, a catheter was implanted into the juglar vein of mice for infusions. Then mice were placed in custom-build animal holders equipped with physiological monitoring and anesthesia delivery. Respiratory monitoring was done using an SA instruments model 1025 MRI compatible physiological monitoring system (Model 1025, SA Instruments, Stony Brook, NY). MRI data were obtained using a 7 Tesla/16 cm Bruker Pharmascan (Karlsruhe, Germany), with a 38 mm volume coil transmitter and receiver. Whole body T_1 weighted images were obtained using 3D FLASH with acquisition parameters of 50 x 40 x 20 mm field-of-view (FOV), a 256 x 196 x 128 matrix, 35° flip angle, 10 ms repetition time (T_R), 2.7 ms echo time (T_E), and six averages for a total acquisition time of 25 m 5.28 s. Images were reconstructed to 256 x 256 x 256.

Mouse MRI Data Analysis using ImageJ. We measure Region of Interest (ROI) using Freehand and Rectangle Selections as shown in an example below.

Freehand Selection ("0107-0108-0094") X: 84 Y: 93 Width: 21 Height: 30	Rectangle Selection ("0107-0109-0087") X: 85 Y: 107 Width: 4 Height: 4	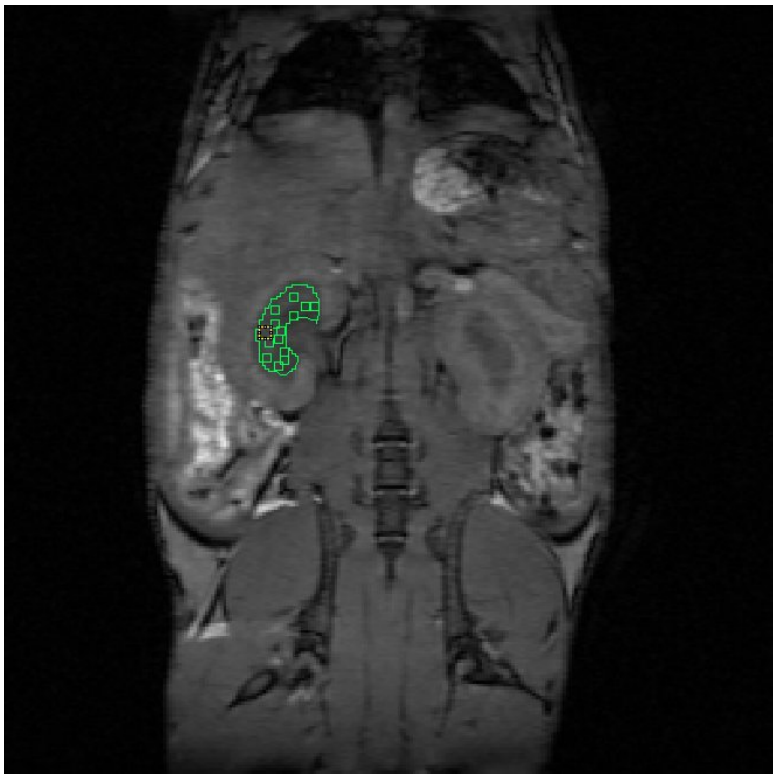

Label	Area	Mean	StdDev	Mode	Min	Max	Circ	IntDen	RawIntDen	Slice	AR	Round	Solidity
2dseq_4_M35:0107-0108-0094:107	346	6399.673	575.321	6770	4700	7731	0.519	2214287	2214287	107	2.088	0.479	0.758
2dseq_4_M35:0107-0109-0087:107	16	6988.312	253.759	6643	6643	7553	0.785	111813	111813	107	1	1.000	1

Label	Area	Mean	StdDev	Mode	Min	Max	Circ	IntDen	RawIntDen	Slice	AR	Round	Solidity
2dseq_4_M35:0107-0101-0090:107	9	6468.556	264.464	5981	5981	6857	0.785	58217	58217	107	1	1.000	1
2dseq_4_M35:0107-0097-0096:107	9	6600.556	160.854	6402	6402	6896	0.785	59405	59405	107	1	1.000	1
2dseq_4_M35:0107-0117-0087:107	9	6640.667	148.082	6414	6414	6869	0.785	59766	59766	107	1	1.000	1
2dseq_4_M35:0107-0120-0091:107	9	6398.444	253.029	5938	5938	6671	0.785	57586	57586	107	1	1.000	1
2dseq_4_M35:0107-0118-0093:107	9	6507.111	253.589	6130	6130	6803	0.785	58564	58564	107	1	1.000	1
2dseq_4_M35:0107-0108-0092:107	9	6394	289.544	5798	5798	6714	0.785	57546	57546	107	1	1.000	1
2dseq_4_M35:0107-0103-0096:107	9	5251.111	189.447	5027	5027	5510	0.785	47260	47260	107	1	1.000	1
2dseq_4_M35:0107-0112-0088:107	9	6916.778	186.480	6765	6765	7245	0.785	62251	62251	107	1	1.000	1
2dseq_4_M35:0107-0115-0093:107	9	5592.778	177.281	5371	5371	5860	0.785	50335	50335	107	1	1.000	1
2dseq_4_M35:0107-0106-0090:107	9	6538.889	185.376	6305	6305	6815	0.785	58850	58850	107	1	1.000	1
2dseq_4_M35:0107-0100-0103:107	9	5974.556	287.192	5673	5673	6557	0.785	53771	53771	107	1	1.000	1
2dseq_4_M35:0107-0100-0100:107	9	5810.889	284.878	5554	5554	6266	0.785	52298	52298	107	1	1.000	1
2dseq_4_M35:0107-0111-0091:107	9	6463.778	286.124	6121	6121	7113	0.785	58174	58174	107	1	1.000	1
Summary:													
Mean	9	6273.701	228.180	5959.923	5959.923	6628.923	0.785	56463.308	56463.308	1	1	1	
SD	0	474.079	54.014	475.669	475.669	487.247	0	4266.711	4266.711	0	0	0	
Min	9	5251.111	148.082	5027	5027	5510	0.785	47260	47260	1	1	1	
Max	9	6916.778	289.544	6765	6765	7245	0.785	62251	62251	1	1	1	

The average mean value (highlighted in blue), obtained from several areas with value of 9, for time 0 (pre-injection), 30 min, 60 min and 90 min, of raw data are tabulated for selected organs (Blood, Kidney-Medulla, Kidney-Cortex, Liver, Muscle Tissue, and Bladder) for each mouse. We normalize the mean values of a selected organ to that of Muscle Tissue which remain nearly constant over the time of the experiment. The mean and standard error of normalized data for 3 mice are plotted in the Figure 4 (main text).

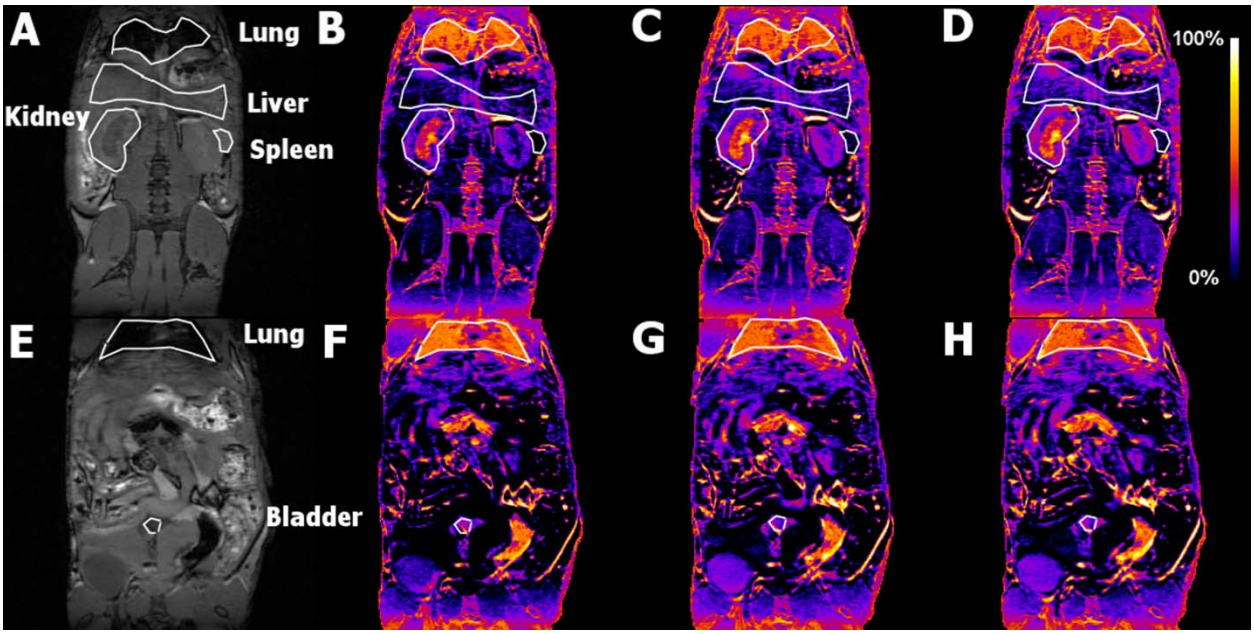

Fig. S25. Enlarged Figure 3 (main text). 3D T_1 weighted spoiled gradient recalled echo MRI of mouse before and after injection of **1**-mPEG-G4. (A,E) MRI before injection and (B–D,F–H): subtraction of pre-injection images from images obtained (B,D) 0–30 min, (C,E) 30–60 min, and (D,H) 60–90 min after injection.

Section 5. Supporting References

1. Ma, Z.; Huang, Q.; Bobbitt, J. M. Oxoammonium salts. 5. A new synthesis of hindered piperidines leading to unsymmetrical TEMPO-type nitroxides. Synthesis and enantioselective oxidations with chiral nitroxides and chiral oxoammonium salts. *J. Org. Chem.* **1993**, *58*, 4837–4843.
2. Rajca, A.; Kathirvelu, V.; Roy, S. K.; Pink, M.; Rajca, S.; Sarkar, S.; Eaton, S. S.; Eaton, G. R. A spirocyclohexyl nitroxide amino acid spin label for pulsed EPR spectroscopy distance measurements. *Chem. Eur. J.* **2010**, *16*, 5778–5782.
3. Sosnovsky, G.; Cai, Z. A Study of the Favorskii rearrangement with 3-bromo-4-oxo-2,2,6,6-tetramethylpiperidine-1-oxyl. *J. Org. Chem.* **1995**, *60*, 3414–3418.

4. Vianello, F.; Momo, F.; Scarpa, M.; Rigo, A. Kinetics of nitroxide spin label removal in biological systems: An in vitro and in vivo ESR study. *Magn. Reson. Imaging* **1995**, *13*, 219–226.
5. Stoll, S.; Schweiger, A. EasySpin, a comprehensive software package for spectral simulation and analysis in EPR. *J. Magn. Reson.* **2006**, *178*, 42–55.
6. Franchi, P.; Lucarini, M.; Pedrielli, P.; Pedulli, G. F. Nitroxide radicals as hydrogen bonding acceptors. An infrared and ESR study. *ChemPhysChem* **2002**, *3*, 789–793.
7. Maliakal, A. J.; Turro, N. J.; Bosman, A. W.; Cornel, J.; Meijer, E. W. Relaxivity studies on dinitroxide and polynitroxyl functionalized dendrimers: effect of electron exchange and structure on paramagnetic relaxation enhancement. *J. Phys. Chem. A* **2003**, *107*, 8467–8475.
8. Borah, B.; Bryant, R. NMR relaxation dispersion in an aqueous nitroxide system. *J. Chem. Phys.* **1981**, *75*, 3297–3300.
9. Nicolle, G. M.; Toth, E.; Schmitt-Willich, H.; Raduchel, B.; Merbach, A. E. The impact of rigidity and water exchange on the relaxivity of a dendritic MRI contrast agent. *Chem. Eur. J.* **2002**, *8*, 1040–1048.